Trends in heat and cold wave risks for the Italian Trentino Alto-Adige region from 1980 to 2018

Martin Morlot[1], Simone Russo[2], Luc Feyen[2], and Giuseppe Formetta[1]

[1] University of Trento, Department of civil, environmental, and mechanical engineering, via Mesiano, 77, 38123, Trento (Italy)

[2] European Commission, Joint Research Centre

Corresponding author: Giuseppe Formetta, giuseppe.formetta@unitn.it

Abstract

Heat waves (HWs) and cold waves (CWs) can have considerable impact on people. Mapping risks of extreme temperature at local scale accounting for the interactions between hazard, exposure and vulnerability remains a challenging task. In this study, we quantify risks from HWs and CWs for the Trentino-Alto Adige region of Italy from 1980 to 2018 at high spatial resolution. We use the Heat Wave Magnitude Index daily (HWMId) and the Cold Wave Magnitude Index daily (CWMId) as the hazard indicator. To obtain HWs and CWs risk maps we combined: i)occurrence probability maps of the hazard, ii) normalized population density maps, and iii) normalized vulnerability maps based on eight socioeconomic indicators. The occurrence probability of the hazard is obtained using the Tweedie zero-inflated distribution. The methodology allowed us to disentangle the effects of each component of the risk to its total change.

We find a statistically significant increase in HWs hazard and exposure while CWs hazard remained stagnant in the analyzed area over the study period. A decrease in vulnerability to extreme temperature spells is observed trough the region except in the

Deleted: G

Deleted: HW)

Deleted: CW)

Formatted: Not Highlight

Formatted ... [1]

Deleted: human …isks from HW …Ws and CW …Ws at high resolution ... [2]

Formatted: English (US)

Deleted: a

Deleted: These are then and as temperature-based indicators andnormalizestandardized it to the interval [0;1]

Deleted: the

Deleted: with the apply a Tweedie zero-inflated distribution distribution to derive hazard intensities and frequencies to . The These normalized hazard maps are combine themd with

Deleted:

Deleted: high-resolution maps of population

Deleted: of density , and…those for which the vulnerability is quantified at community and city level using a set of eight ... [3]

Formatted: Not Highlight

Deleted: s

Deleted: combined in order to obtain risk maps… The occurrence probability standardization …f the hazard is performed…btained with ... [4]

Deleted:

Deleted: HW

Deleted: those of

Deleted: , with 6.0-times more people exposed to extreme heat after 2000 compared to the last two decades of the previous century.

Deleted:

Deleted: CW …Ws hazard hazard and exposure ... [5]

Deleted: ied

Deleted: period in the region

Deleted: We observe a

Deleted: general trend towards increased resilience…ecrease in vulnerability to extreme ... [6]

Formatted: Not Highlight

Deleted: trend …s observed trough the regiondue ... [7]

Deleted: over the region

Deleted: . However, In in the region's

Deleted: the

larger cities where vulnerability has increased. HWs risk increased in 40% of the region, with it being stronger in highly populated areas. Stagnant CWs hazard and declining vulnerability result in reduced CWs risk levels, with exception of the main cities where it grew due to their increased vulnerabilities and exposures.

The findings of our study are relevant to steer investments in local risk mitigation, and this method can potentially be applied to other regions that have similar detailed data.

1 Introduction

Heat waves (HWs) and cold waves (CWs) are hazards that affect public health and the environment (Gasparrini et al., 2015; Habeeb et al., 2015). With global warming, HWs intensities and durations are expected to increase while those of CWs are expected to decrease (Perkins-Kirkpatrick and Gibson, 2017; Russo et al., 2015; Smid et al., 2019), which would change their risks to society. A recent report showed that in the year 2018, worldwide, 157 million more people were exposed to HWs compared to the year 2000 (Watts et al., 2018). In Europe, recent high intensity HWs events (2003 and 2018, where HWs are defined as 3 days over 90th temperature percentile of the 1980-2010) have impacted as much as 55% of its area (García-León et al., 2021). In Italy, HWs have had a strong impact on mortality such as in 2003 when a 27% mortality increase was reported over August, while in 2015 there was a 23% increase in July, compared to the 5 previous years (Michelozzi et al., 2005, 2016). In Trentino Alto-Adige (our study region), Conti et al. (2005) showed that for the large HW of 2003, mortality increased by 32% in Trento and 28% in Bolzano (the region's two main cities) compared to the

Deleted: of the region
Deleted: ,
Deleted: however, we find that
Deleted: due to an ageing population and more single households
Deleted: HW
Deleted: has risen
Deleted: practically everywhere
Deleted: the XX…0% of the region, with it being stronger in highly populated areas, indicating that even the reductions in vulnerability in the smaller communities is are outpaced by the increase in HW HWs hazard and exposure … [8]
Deleted: In the large cities, HW risk levels in the 2010s are 50% larger compared to the 1980s due to the rise in both hazard and vulnerability. …Whereas in smaller communities, s…tagnant CW …Ws hazard and declining vulnerability results …esult in reduced CW CWs risk levels, with exception of the main,…the risk level in …ities where it grew due to their increased vulnerabilities and exposures.cities grew … [9]
Deleted: by 20% due to the increased vulnerability over the study period. …he findings of our study are highly relevant for steering…o steer investments in local risk mitigation measures… and , while the…his method can potentially be applied to other regions that have similar detailed information…ata on hazard, exposure and vulnerability indicators … [10]
Deleted: HW)…Ws) and cold waves (CW) …Ws) are hazards that affect public health and the environment (Gasparrini et al., 2015; Habeeb et al., 2015). With global warming, HWs intensities and durations heat and cold wave intensities and durations …re expected to change…xpected to increase while those of CWs … [11]
Deleted: ,…worldwide, 157 million more people v … [12]
Formatted: English (US)
Formatted … [13]
Deleted: …5% of the … [14]
Deleted: of Europe was impacted by HW over th … [15]
Deleted: With regards to CW in Europe, recent w … [17]
Formatted: Not Highlight
Formatted … [16]
Field Code Changed
Deleted: and a 6% increase during the summer … [18]
Deleted: the T…rentino Alto-Adige region …the … [19]
Deleted: heat wave
Deleted: of the region
Deleted: with

previous year. In the city of Bolzano, it was also found that higher hospital admissions occurred during HWs events particularly among elderly women (Papathoma-Köhle et al., 2014). With regards to CWs in Europe, recent winters have claimed 790 deaths in 2006 and 549 deaths in 2012 (Kron et al., 2019). The increase in mortality and among the elderly people is also found in Italy for CWs. For example, de'Donato et al., (2013) reported a notable increase in mortality (47%) for the timeframe of the 2012 CW in the city of Bolzano.

HWs and CWs events clearly come with a risk but how do we define this risk? The United Nations Office for Disaster Risk Reduction (UNDRR, 2021) and the Intergovernmental Panel on Climate change (IPCC, 2014) define risk as a function of hazard, exposure, and vulnerability. Exposure is defined as people, infrastructure, housing, production, and other tangible human assets present in hazard-prone areas. Vulnerability is defined as the conditions that define the susceptibility of an individual, infrastructure, or a community to be impacted by the hazard. To successfully quantify risk, one must be able to measure all three components: hazard, exposure, and vulnerability.

With regards to hazard and exposure, several temperature hazard-exposure studies have been conducted at global (e.g. Chambers, 2020; Dosio et al., 2018), continental (eg. King et al., 2018), or city-scale (e.g. Smid et al., 2019). Most studies focus on human exposure (eg. Chambers, 2020; Tuholske et al., 2021) and on the exposure of land areas (e.g., Ceccherini et al., 2017; Oldenborgh et al., 2019; Russo et al., 2016). These studies found increasing trends in HWs (Chambers, 2020; Dosio et al., 2018)

Deleted: in the city

Deleted: the

Deleted: For Bolzano, Papathoma-Köhle et al.(2014) found that higher hospital admissions in the city occurred during the 2003 HW when comparing it to other years (2006, 2009), particularly among elderly women. …

Deleted:

Deleted: the case of

Deleted: , this was the case during

Deleted: the CW CW of 2012 (de'Donato et al., 2013), with notably an increase

Deleted: of

Deleted: cold spell

Deleted: As has been shown in the previous paragraph,

Deleted: what is a

Deleted: ¶

Formatted: Not Highlight

Formatted: Not Highlight

Deleted: S

Formatted: English (US)

Formatted: English (US)

Deleted:

Formatted: English (US)

Formatted: English (US)

Field Code Changed

Deleted: , but also

Formatted: English (US)

Formatted: English (US)

Deleted: Most of t

Deleted: have

Deleted: exposure to HW

Formatted: Not Highlight

Formatted: Not Highlight

Formatted: English (US)

Formatted: Not Highlight

and decreasing trends in CWs in their period of analysis (Oldenborgh et al., 2019, Smid et al., 2019).

Most studies on HWs and CWs have used qualitative numerical thresholds on the indicator to define severity and exposure to the hazards. However, extreme events are usually defined by their return periods. In the case of HWs and CWs fitting extreme value distributions to define the return periods is difficult due to the possible absence of events in the analyzed time frame (i.e. zero values, in the case where there are no HWs/CWs in a given year). Generalized extreme value distribution (GEV) and non-stationary-techniques (Dosio et al., 2018; Kishore et al., 2022; Russo et al., 2019) have enabled to estimate HWs and CWs' return periods, but both approaches did not explicitly account for the zero presence in the analyzed time series.

Instead, for the first time we use the zero-inflated distribution of Tweedie families (Jorgensen, 1987; Tweedie, 1984) to estimate HWs and CWs frequency of occurrence, which enabled us to directly account for the possible zero values. The Tweedie distribution has been used mostly for the purpose of insurance claims analysis, but has seldom been applied in the field of natural hazards, such as HWs mortality (Kim et al., 2017), droughts (Tijdeman et al., 2020), and rainfall analysis (Dunn, 2004; Hasan and Dunn, 2011). The main advantage of the Tweedie distribution is the possibility of considering many distributions for the continuous and semi-continuous domain such as: normal, Gamma, Poisson, Compound Gamma-Poisson, and Inverse Gaussian (Bonat and Kokonendji, 2017; Rahma and Kokonendji, 2021; Shono, 2008; Temple, 2018). Moreover, for some of these distributions (i.e. Poisson mixtures of gamma distributions) it explicitly enables the fitting of zero-inflated data. Tweedie distribution main limitation is

Deleted: and for the studies that
Deleted: also analyzed CW,
Deleted: when the latter's analysis is present
Formatted: Not Highlight
Formatted: Not Highlight
Deleted: found decreasing trends for them.
Formatted: Not Highlight
Deleted: Typically,
Deleted: Usually, t…osthese … [20]
Deleted: these
Deleted: previous…studies on HWs and CWs on on the topicHWs and CWs, … [21]
Deleted: however relied on using…sed qualitative numerical thresholds on the indicator to define … [22]
Deleted: of
Deleted: the severity of the events and define exposure according to these thresholds… However, … [23]
Deleted: HW
Deleted: HWs and CW CWs
Deleted: hazards
Deleted: can also be
Deleted: normally
Deleted: but
Deleted: these
Deleted: for multiple years in their time series… … [24]
Deleted: Generalised…eneralized extreme value distribution (GEV) and non-stationary-techniques (Dosio et al., 2018; Kishore et al., 2022; Russo et al., 2019) have enabled to estimate HW … [25]
Deleted: s
Deleted: circumvent this absence rather than considering …he zero values directly … [26]
Deleted: statistical …ime series.¶ … [27]
Deleted:
Deleted: We…we therefore …se for the first time …he zero-inflated distribution form … [28]
Deleted: HW …Ws and CW … [29]
Deleted: s for the direct fitting…irectly account for of the possible zero values. The Tweedie distribution has been used mostly for the purpose of insurance cl… [30]
Deleted: One of the advantages of the Tweedie … [31]
Deleted: Some of th…he main e … [32]
Deleted: advantage
Deleted: s…of the Tweedie distribution is the pos… [33]

the complex distribution's fitting methodology and the difficulties to compare it to other models via information criteria such the Akaike's information criterion (Shono, 2008).

To perform a risk analysis, the vulnerability to the hazard must be quantified. HWs and CWs vulnerabilities can be approximated by combinations of several socioeconomic indicators. At the community level in the United States, factors such as social isolation, presence of air conditioning, proportion of elderly and proportion of diabetics in the population were found to be key for human vulnerability to temperature extremes (Reid et al., 2009). In Korea at the county level, Kim et al. (2017) found that elderly living alone, agricultural workers and unemployed are the main indicators for vulnerability to heat wave days and tropical nights. Temperature vulnerability has also been appraised at city scale for HWs mortality (Ellena et al., 2020) and at regional scale (López-Bueno et al., 2021) for CWs mortality. Karanja & Kiage (2021) and Cheng et al. (2021) provide an overview of the different types of indicators used in the literature to quantify vulnerability. The indicators can be diverse, ranging from population structure (e.g., age and health characteristics), social status, economic conditions, community (cultural) group characteristics, and household physical characteristics. Studies on social vulnerability to natural hazards in Italy used a diversity of indicators derived from the census records (Frigerio and De Amicis, 2016).

HWs and CWs risks are often assessed using different methodologies depending on the objectives of the study. On a global scale, Russo et al., (2019) establish a risk index using the probabilities of HWs as hazard, where the exposure is the population density normalized in [0;1] based on its maximum, minimum values; while vulnerability is based on a socio-economic indicator (human development index). For Italy, Morabito et al

Deleted: that
Deleted: and properties render complicated
Deleted: the comparison
Deleted: estimate of values or
Deleted: one must know
Deleted: also be known
Deleted: To this end, the vulnerabilities to temperature extremes are complex to quantify.
Deleted: Recent studies have developed temperature-mortality relationships (e.g., Gasparrini et al., 2015) at the scale of cities. However, this requires that the city has substantial population, and sufficiently long records of mortality and temperature. HW
Formatted: English (US)
Formatted: English (US)
Deleted: CW
Deleted: y
Deleted: also
Deleted: the
Deleted: affect
Deleted: HW
Deleted: CW
Deleted: characterize
Deleted: e.g.
Deleted: Work
Deleted: has
Deleted: found in
Deleted: Other analyses conducted for Italian cities focused on neighborhood and building levels to produce HW HWs vulnerabilities for Milano (Bhattacharjee ... [34]
Formatted: Italian
Formatted: Italian
Field Code Changed
Deleted: With regards to the overall
Deleted: The
Deleted: of
Deleted: HW
Deleted: HWs and CW CWs, these
Deleted: ,
Deleted: HW
Deleted: normalized
Deleted: and

(2015) conducted a risk analysis of heat on elderly in the major cities, using the elderly population as the only vulnerability factor and summer average temperatures for the period 2000-2013 to quantify the hazards.

Assess the risk associated to extreme temperatures in the Italian Trentino Alto-Adige region is a relevant social and scientific objective given: i) the increase in the percentage of elderly people (i.e. vulnerability change) (Papathoma-Köhle et al., 2014) and ii) the changing temperature extremes in view of climate change (i.e. changing hazard).

Few studies have attempted to quantify HWs and CWs impacts for the Trento and Bolzano cities (main cities of the region), such as Conti et al. (2005) as part of their studies on Italian cities and Papathoma-Köhle et al. (2014) who studied impacts in Bolzano. The former compared the mortality data of the year 2003 (affected by the very intense HW) to the year 2002, finding an increase of morality in both Trento and Bolzano. The latter compared the hospital admissions due to HWs in summer months of three years (2003, 2006, and 2009) possible heat health issues among elder women.

To better understand the spatiotemporal evolution of HWs and CWs human risk and to plan adequate risk-mitigation measures in the region, there is a need to assess the risk and its change at high spatial and temporal resolution.

The aim of this article is to solve some of these previous limitations while quantifying HW and CW hazards, the human exposures, vulnerabilities, and risks at the high-definition (i.e. city-scale) over the period 1980-2018, for the Trentino-Alto-Adige region. The goals for this paper are therefore as follow:

Deleted: The

Deleted: of Italy is composed of two provinces (Trento and Bolzano). It is a region

Deleted: of interest to study HW HWs and CW CWs risks due to an expected

Deleted: number and

Deleted: ,

Deleted: which in combination with

Deleted: increasing

Deleted:

Deleted: could increase human risks (Bacco and Scorzini, 2020)…

Deleted: HW

Deleted: CW

Deleted: cities in the region (e.g. Trento and Bolzano

Deleted:),

Deleted: The findings of these study are limited for two reasons: they use few samples per day (Papathoma-Köhle et al., 2014) and short timeframes, e.g., comparing only 2002 to 2003 in Conti et al. (2005) and considering only 4 years of data in Papathoma-Köhle et al. (2014). However, conducting spatial-temporal risks analyses of HW HWs and CW CWs are typically not done over a large timeframe at such a detailed location scale (city-level); yet these are important to forge a better understanding of the spatiotemporal human risks and their underlying drivers which are critical to plan risk-mitigation measures at the local level.¶

Deleted: heat and cold waves

Deleted: y

Deleted: for the

Deleted:

Deleted: over the period 1980-2018

Deleted: The quantification of the hazard and its return period will be performed using the Heatwave magnitude index HWMId and its cold wave counterpart CWMId (Russo et al., 2014, 2015) and using the novel method of fitting the Tweedie distribution to help us estimate the exposure and risk.

1) Quantify HWs and CWs hazards and their return level at a very high spatial resolution (250m) by combining for the first time i) the indicators proposed by Russo et al. (2015) and Smid et al. (2019), together with ii) the Tweedie distribution;

2) Quantify human exposures and vulnerabilities to HWs and CWs and their evolution in time for the Trentino-Alto-Adige region;

3) Quantify the HWs and CWs risks across the region and understand their main drivers by disentangling the contribution of the risks' components to its change.

2 Study Area

The Trentino Alto-Adige region (Figure 1: The Trentino Alto-Adige region and its most populated cities (Trento, Bolzano, Rovereto and Merano); the colors indicating the elevations, river network, and lakes.

) is a mountainous region in northern Italy, which borders Austria. The elevation of the region varies from 65m for lake Garda to 3,439m for Lagaunspitze. It is composed of two provinces (Province of Trento and Province of Bolzano). Its most populous cities (population for 2022 in parenthesis) are the two provincial capitals, Trento (118509) and Bolzano (107025), as well as minor cities such as Merano (40994) and Rovereto (39819). The main rivers in the region are the Adige, and its tributary, the Isarco. Due to its diverse geography, the climate is also diverse ranging from Subcontinental to Alpine on the Koppen classification (Fratianni and Acquaotta, 2017).

Deleted: ,
Deleted: ,
Deleted: using HWMId, CWMId
Deleted: and
Deleted: at a very high spatial resolution
Deleted: exposur
Deleted: e
Deleted: y
Deleted: events
Deleted: risk to
Deleted: s of past HWs and CWs events an
Deleted: d
Deleted: which were the main underlying components to these risks
Deleted: ¶
Formatted: Font colour: Auto
Formatted: Font colour: Auto
Formatted: Line spacing: Double

Deleted: Figure *1*
Deleted: (¶
Figure *1*: The Trentino Alto-Adige region)
Formatted: English (US)

Deleted: Its most populous cities are the two provincial capitals -- Trento and Bolzano -- as well as minor cities Merano and Rovereto (both have a population of over 30000).

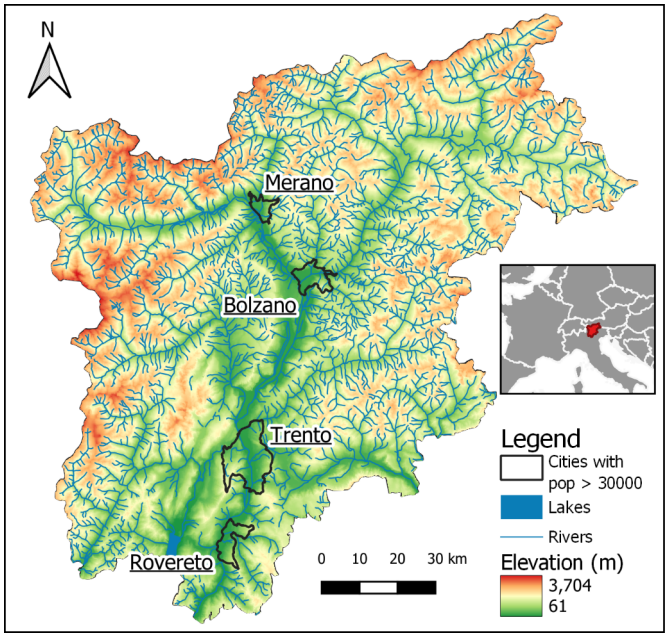

Figure 1: The Trentino Alto-Adige region and its most populated cities (Trento, Bolzano, Rovereto and Merano); the colors indicating the elevations, river network, and lakes.

3 Methodology

3.1 Temperature data

In order to quantify the HWs and CW hazard, we used the freely available spatial temporal temperature dataset by Crespi et al. (2021). It consists of gridded daily temperatures for the entire Trentino Alto-Adige region covering the period of 1980-2018 at a resolution of 250 meters. This dataset is based on more than 200 station daily records which have been quality controlled and homogenized. The interpolation method is based on a combination of 30-year temperature climatology (1981–2010), daily

Formatted: Font colour: Auto
Formatted: Font colour: Auto
Formatted: Font colour: Auto
Formatted: Line spacing: Double
Deleted: Figure 1: The Trentino Alto-Adige region, its most populated cities (Trento, Bolzano, Rovereto and Merano) and the colors indicating the elevations; river network and lakes
Deleted: Figure 1: The Trentino Alto-Adige region¶
Deleted: HW
Formatted: Line spacing: Double
Formatted: Font: (Default) +Body (Arial), Font colour: Auto

anomalies and explicitly accounts for topographic features (i.e. elevation, slope) which are crucial in orographic complex areas such as the Trentino Alto-Adige. The leave one out cross validation presented in Crespi et al. (2021) finds mean correlation coefficient higher than 0.8 and mean absolute errors of around 1.5 degree Celsius (on average across months and stations used for the interpolation).

The hazard analysis presented in this paper rely on the Crespi et al. (2021) air temperature database. Although it is based on a state-of-the-art interpolation approach and it represents the best product for the area, more attention should be given to measuring meteorological variables in orographically complex area and at high elevation. This will in turn reduce the uncertainty in spatial interpolation and improve the quantification of impacting hazards such as HWs and CWs.

3.2 Hazard quantification and distribution fitting

3.2.1 Hazard quantification

To quantify the hazard we used the HWMId (Russo et al., 2015) and the CWMId (Smid et al., 2019). These indices represent a way of measuring extreme temperature events while considering their durations, intensity, and taking in account the site-specific historical climatology (30years).

According to Russo et al. (2015), HWMId is defined as the maximum magnitude of the HWs in a year. A HW occurs when the air temperature is above a daily threshold for more than three consecutive days. The threshold is set to the 90th percentile of the temperature data of the day and the window of 15 days before and after throughout the reference period 1981-2010. The magnitude of a HW is the sum of the daily heat magnitude HM_d of all the consecutive days composing the HW (Equation 1):

Deleted: The hazard analysis presented in this paper rely on the Crespi et al. (2021) air temperature database. Although it is based on a state-of-the-art interpolation approach and it represents the best product for the area, more attention should be given to measuring meteorological variables in orographic complex area and at high elevation. This will in turn reduce the uncertainty in spatial interpolation and improve the quantification of impacting hazards such as HWs and CWs

Deleted: The dataset is obtained with the anomaly-based approach taking into account elevation of the local station observations; the dataset has undergone a quality analysis and control against the stations' observations (Crespi et al. 2021).

Deleted: ,

Deleted: and sizing

Formatted: Font: (Default) +Body (Arial)

Formatted: Heading 3

Formatted: Font: (Default) +Body (Arial), Font colour: Auto

Formatted: Font: (Default) +Body (Arial), Font colour: Auto

Formatted: Line spacing: Double

Formatted: Font: (Default) +Body (Arial), Font colour: Auto

Formatted: Font colour: Auto

Formatted: Font colour: Auto

Formatted: Font: (Default) +Body (Arial), Font colour: Auto

$$HM_d(T_d) = \begin{cases} \frac{T_d - T_{30y25p}}{T_{30y75p} - T_{30y25p}} & \text{if } T_d > T_{30y25p} \\ 0 & \text{if } T_d \leq T_{30y25p} \end{cases} \quad (1)$$

where $HM_d(T_d)$ corresponds to the daily heat magnitude, T_d the temperature of the day in question and T_{30y25p} and T_{30y75p} correspond to the 25th and 75th percentile of the yearly maximum temperature for the 30 years of the reference period (1981-2010). The interquartile range (IQR, i.e. the difference between the T_{30y75p} and T_{30y25p} percentiles of the daily temperature) is used as the heatwave magnitude unit and represents a non-parametric measure of the variability of the temperature timeseries. Therefore, a value of HM_d equals to 3 means that the temperature anomaly on day d with respect to T_{30y25p} is 3 times the IQR. Finally, for a given year HWMId corresponds to the highest sum of magnitude (HMd) over the consecutive days composing a heatwave event (with only days with HMd > 0 considered).

Analogously to the HWMId, CWMId is defined as the minimum magnitude of the CWs in a year (Smid et al., 2019). A CW occurs when the air temperature is below a daily threshold for more than three consecutive days. The threshold is set to the 10th percentile of the temperature data of the day and the window of 15 days before and after throughout the reference period 1981-2010.

The daily cold magnitude corresponds to (Equation 2):

$$CM_d(T_d) = \begin{cases} \frac{T_d - T_{30y75p}}{T_{30y75p} - T_{30y25p}} & \text{if } T_d < T_{30y75p} \\ 0 & \text{if } T_d > T_{30y75p} \end{cases}$$

Formatted ... [35]

Formatted ... [36]

Formatted ... [37]

(2)

where $CM_d(T_d)$ corresponds to the cold daily magnitude, T_d the daily temperature and T_{30y25p} and T_{30y75p} correspond to the 25th and 75th percentile yearly temperature for the 30 years used as a reference. Inversely to HWMId, the lowest cumulative magnitude sum is retained for each year and with only consecutive days with $CM_d < 0$ considered to calculate it. CWMId being always <T 0, its absolute values are retained for its values to be on a positive interval (similar to HWMId).

3.2.2 Distribution fitting

The HWMId and CWMId yearly values are fitted with a probability distribution to estimate their return periods. Considering that HWMId and CWMId are both defined in [0,+Inf[, we use the Tweedie distribution (Jorgensen, 1987; Tweedie, 1984), a distribution that can act as zero-inflated, thus accounting for the presence of zeros directly. The Tweedie distribution is an exponential dispersion model which has a probability density function of the form (equation 3):

$$f(y,\theta,\Phi) = a(y,\Phi) * \exp\left[\frac{1}{\Phi}\{y\theta - \kappa(\theta)\}\right] \quad (3)$$

where Φ corresponds to its dispersion parameter that is positive, θ to its canonical parameter, and $\kappa(\theta)$ the cumulant function. The function a(y, Φ) generally cannot be written in closed form. The cumulant function is related to the mean ($\mu_y = \kappa'(\theta)$) and variance ($\sigma_y = \Phi * \kappa''(\theta)$) and in the case of a Tweedie distribution the variance has a power relationship with the mean (Equation 4):

Deleted: To quantify the hazard we used the HWMId (Russo et al., 2015) and the CWMId (Smid et al., 2019). These indices represent by their methodology a way of measuring extreme temperature events while considering their durations, intensity, specific locations while taking in account the historical extremes (30years) of the specific location. These are calculated by the methodology that follows.¶
According to Russo et al. (2015), HWMId is defined as the maximum magnitude of the HWs in a year. A HW occurs when the air temperature is above a daily threshold for more than three consecutive days. The threshold is set to the 90th percentile of the temperature data of the day and the window of 15 days before and after throughout the reference period 1981-2010. The magnitude of a HW is the sum of the daily heat magnitude HM_d of all the consecutive days composing the HW (equation 1):¶

$$HM_d(T_d) = \begin{cases} \frac{T_d - T_{30y25p}}{T_{30y75p} - T_{30y25p}} & \text{if } T_d > T_{30y25p} \\ 0 & \text{if } T_d \leq T_{30y25p} \end{cases} \quad (1)$$¶

where HMd(Td) corresponds to the daily heat magnitude, Td the temperature of the day in question and T30y25p and T30y75p correspond to the 25th and 75th percentile of the yearly maximum temperature for the 30 years of the reference period (1981-2010). The interquartile range (IQR, i.e. the difference between the T30y75p and T30y25p percentiles of the daily temperature) is used as the heatwave magnitude unit and represents a non-parametric measure of the variability of the temperature timeseries. Therefore, a value of HM_d equals to 3 means the temperature anomaly on day d with respect to T30y25p is 3 times the IQR. Finally, for a given year HWMId corresponds to the highest sum of magnitude (HMd) over the consecutive days composing a heatwave event with only days with HMd > 0 considered. ¶ ... [38]

Deleted: sizing of

Deleted: quantification

Deleted: ¶

Formatted: Font: (Default) +Headings (Arial), Font colour: Auto

Formatted: Font: (Default) +Headings (Arial), Font colour: Auto

Deleted: To quantify the hazard, we used HWMId (Russo et al., 2015) and CWMId (Smid et al., 201 ... [39]

Deleted: The values can then be modelled with a specific probability distribution to estimate the return periods of HW and CW.

Formatted: Font: (Default) +Body (Arial)

Deleted: 4

Deleted: 4

Deleted: 5

$$\sigma_y = \Phi * (\mu_y)^p \quad (4)$$

where p corresponds to the power parameter that is positive.

Depending on the value of p, the distribution will behave differently. In the case where p is between 1 and 2, it belongs to the compound Poisson-gamma distribution with a mass at zero, while other p values can make the distribution correspond to a normal, Poisson, or gamma distribution, among others. The use of the Tweedie distribution is retained as it permits to consider the zero values, while also considering other distributions should there be an absence of zero values.

We fit the distribution to the previously found HWMId and CWMId values with the help of the Tweedie R package (Dunn, 2021). It provides distribution density, distribution function, quantile function, random generation for the Tweedie distributions. The Tweedie parameters (i.e. mean, power, and dispersion) have been estimated by the "tweedie.profile" function (Dunn, 2015) using the maximum likelihood as described by Dunn (2015) and Dunn and Smyth (2005). An example of the fitted distribution for Bolzano and Trento can be found in the supplementary material (Figure S1). It is also possible to use the same package to estimate a quantile using the fitted distribution. This enables to estimate specific return levels for return periods T for both HWMId and CWMId. For this study two return levels are retained, 5 years (HW5Y for HW, and CW5Y for CW) and 10 years (HW10Y for HWs and CW10Y for CW). This choice aims to account for of both the length of the analyzed period (39 years) and the type of hazards we are analyzing (HWs and CWs usually doesn't occur every year). Higher

Deleted: 5

Formatted: Font: (Default) +Body (Arial)

Formatted: Font: (Default) +Body (Arial), Font colour: Auto

Field Code Changed

Deleted: –

Deleted: HW

Formatted: Font: (Default) +Body (Arial), Font colour: Auto

return level estimations would be affected by extrapolation effects and higher uncertainty.

For statistical fit verification, the Kolmogorov–Smirnov (KS) test on two samples is used with one sample being the found HWMId or CWMId values, and the other sample being a randomly generated sample using the fitted distribution value. This goodness of fit of test is one of the most commonly used in the literature for the case of the corresponding zero inflated Tweedie distribution (Goffard et al., 2019; Johnson et al., 2015; Rahma and Kokonendji, 2021). The null hypothesis of this test is that the two sample belong to the same distribution. If the P-value for this test is below the significance level α of 5%, the null hypothesis is rejected, otherwise we cannot reject the null hypothesis at this significance level.

3.3 Exposure quantification

To quantify the population exposed to HWs and CWs, we use time-varying population data from the Global Human Settlement Layer (GHSL) (Schiavina et al., 2019). The population data is available at a resolution of 250m for the following years: 1975, 1990, 2000 and 2015. Both this data, and the population count done by the Italian national statistical institute, indicate a growing population throughout the region (overall 23%).

To more accurately model exposure, we created yearly varying population maps for the period 1980-2018 following the methodology presented in other studies (e.g. Formetta and Feyen, 2019; (Neumayer and Barthel, 2011). We linearly interpolated the data in time for the period 1980 to 2015 (assuming a constant rate in between available years) and we used the closest year for the period 2016-2018.

Formatted: Default Paragraph Font

Formatted: Font: (Default) +Body (Arial)

Formatted: Font: (Default) +Body (Arial)

Formatted: Font: (Default) +Body (Arial), Font colour: Auto

Formatted: Line spacing: Double

Formatted: Font: (Default) +Body (Arial), Font colour: Auto

Following recent studies (King & Harrington, 2018; Russo et al., 2019), for each year, a pixel is considered exposed to HW/CWs hazard (or to a 5 or 10 year return-period HWs/CWs) if for that year the HWMId/CWMId of the pixel is greater than zero (or greater than the corresponding return level HW5Y/CW5Y or HW10Y/CW10Y, respectively).This is the exposition factor, and it is a binary value (0 meaning not exposed or 1 meaning exposed).

The percentage of population exposed are calculated on annual basis over the study period (1980-2018) with the help of population data linearly interpolated from 1980 to 2018.

Using this population data, percentage of population exposed are then calculated using the following equation (Equations 5 and 6):

$$Population\ exposed(t) = \sum EF_i * population_i(t) \quad (5)$$

$$Percentage\ of\ population\ exposed\ (t) = \frac{Population\ exposed(t)}{Total\ population\ (t)} \quad (6)$$

where i corresponds to the pixels, t to the year being analyzed, EF to the exposition factor mentioned above (binary).

3.4 Vulnerability quantification

We express HWs and CWs vulnerability using eight indicators as in Ho et al. (2018), who quantify community vulnerability to HWs and CWs events based on extreme age,

Deleted: e
Formatted: Font: (Default) +Body (Arial), Font colour: Auto
Formatted: Font: (Default) +Body (Arial), Font colour: Auto
Formatted: Font: (Default) +Body (Arial), Font colour: Auto
Formatted: Font colour: Auto
Formatted: Font: Font colour: Auto
Formatted: Font: Font colour: Auto
Formatted: Font: Font colour: Auto
Formatted: Font: Font colour: Auto
Formatted: Font: Font colour: Auto
Formatted: Font: Font colour: Auto
Formatted: Font: Font colour: Auto
Formatted: Font: (Default) +Body (Arial), Font colour: Auto
Formatted: Font: (Default) +Body (Arial), Font colour: Auto
Formatted: Font colour: Auto
Formatted: Font colour: Auto
Formatted: Font colour: Auto
Formatted: Font colour: Auto
Formatted: Font: (Default) +Body (Arial), Font colour: Auto
Formatted: Font: (Default) +Body (Arial), Font colour: Auto
Deleted: Following recent studies (King and Harrington, 2018; Russo et al., 2019), for each year of the time period a pixel is considered exposed if the HW/CW hazard (measured by HWMId or CWMId) is greater than zero or a specified return level value. For that year, the population exposed in the region is the sum of all exposed pixels in the region. The percentage of population exposed is obtained dividing the population exposed by the total population in the region at that time. The results for the percentage of population exposed are calculated on annual basis over the study period (1980-2018).
Deleted: HW
Deleted: CW
Formatted: Line spacing: Double
Deleted: HW
Deleted: CW

household physical characteristics, social status and economic conditions. The list of variables considered are reported in Table 1.

Table 1: Vulnerability indicators used (after Ho et al., 2018)

Category	Indicator	Definition
Extreme Age	Older Age	Population over 55 years old
	Infants	Population under 5 years old
Household physical characteristics	People in old houses	Percentage of household living in housing built prior to 1960 (corresponding to when better insulation started being implemented)
	People in poor living condition	Percentage of household living in other type of housing not meant for inhabitation (cellar, attics)
Social Status	Low education population	Population with low education (no middle-school diploma)
	People living alone	Number of single-person households

Deleted: ¶
Page Break

Deleted: Category ... [40]

Formatted: Font: (Default) +Body (Arial), Font colour: Auto

Formatted: Font: (Default) +Body (Arial), Font colour: Auto

Formatted: Font: (Default) +Body (Arial), Font colour: Auto

Formatted: Font: (Default) +Body (Arial), Font colour: Auto

Formatted: Font: (Default) +Body (Arial), Font colour: Auto

Formatted: Font: (Default) +Body (Arial), Font colour: Auto

Formatted: Font: (Default) +Body (Arial), Font colour: Auto

Formatted: Font: (Default) +Body (Arial), Font colour: Auto

Formatted: Font: (Default) +Body (Arial), Font colour: Auto

Economic Status	Low-income population	Population in a household with children and no money-earning members
	Unemployed	Unemployment rate

The spatially varied indicators are freely available in the census records (i.e. sub-city level) from the Italian national statistical institute (ISTAT, 2021 for three different years (1991, 2001 2011). Given the data time constraints, vulnerability is thus derived for those years only.

The methodology to quantify vulnerability uses the equal weight analysis (EWA, e.g. Liu et al, 2020). Firstly, the individual indicators are standardized between 0 and 1, prior to aggregation (their sum); the standardization is done at the city level for all the years of record (1991, 2001, 2011) based on Equation 7:

$$\text{Standardized Indicator}\ (t) = \frac{\text{Indicator}(t) - \min(\text{Indicator}_{1991,2001,2011})}{\max(\text{Indicator}_{1991,2001,2011}) - \min\ (\text{Indicator}_{1991,2001,2011})} \quad (7)$$

Secondly, the EWA is performed according to Equation 8:

$$\text{Vulnerability}\ (t) = \frac{\sum \text{Standardized indicator(t)}}{\text{number of indicators}} \quad (8)$$

Deleted: Istat.it - 15° Censimento della popolazione e delle abitazioni 2011, 2021)
Formatted: Font: (Default) +Body (Arial)
Formatted: Font: (Default) +Body (Arial), Font colour: Auto
Formatted: Font: (Default) +Body (Arial), Font colour: Auto
Formatted: Line spacing: Double
Formatted: Font: (Default) +Body (Arial), Font colour: Auto
Formatted: Font colour: Auto
Formatted: Font colour: Auto
Formatted: Font colour: Auto
Formatted: Font colour: Auto
Formatted: Font colour: Auto
Formatted: Font colour: Auto
Formatted: Font colour: Auto
Formatted: Font colour: Auto
Formatted: Font colour: Auto
Formatted: Font colour: Auto
Formatted: Font colour: Auto
Formatted: Font colour: Auto
Formatted: Font colour: Auto
Formatted: Font colour: Auto
Formatted: Font colour: Auto
Formatted: Font: (Default) +Body (Arial), Font colour: Auto
Formatted: Right, Line spacing: Double
Formatted: Line spacing: Double
Formatted: Font colour: Auto
Formatted: Font colour: Auto
Formatted: Font colour: Auto
Formatted: Font colour: Auto
Formatted: Font colour: Auto
Formatted: Font: (Default) +Body (Arial), Font colour: Auto
Formatted: Right, Line spacing: Double

This approach was chosen as it is the simplest method for weighing the vulnerability indicators and it is commonly applied in the literature with regards to HWs and CWs (e.g. Buscail et al., 2012; Buzási, 2022).

Finally, we created yearly varying vulnerability maps for the period 1980-2018 following the same approach we used for the population.

3.5 Risk Quantification

Risk here is assumed to be a function of hazard, exposure and vulnerability, which are multiplied to quantify risk (UNDRR, 2021). This is one of the two most commonly used approaches in literature (Dong et al., 2020; Quader et al., 2017; Russo et al., 2019), with the other approach being the addition of the different risk components. Multiplication when compared to addition is found to better highlight the complex relationship between the different components, as the multiplication of the multivariate probabilities of independent variables follow a product law (El-Zein and Tonmoy, 2015; Estoque et al., 2020; Peng et al., 2017).

The risk is calculated as per Dong et al. (2020) (equation 9):

$$\text{Risk} = \sqrt[3]{\text{Hazard} * \text{Exposure} * \text{Vulnerability}} \quad (9)$$

with each of the risk components having a value in [0,1]. The hazard is computed as the probability of occurrence of HWs/CWs by using the fitted Tweedie distributions probability function for each pixel. Exposure is the standardized population density. The vulnerability derived from standardized variables is also between [0,1]. The resulting risk

Formatted: Line spacing: Double

Formatted: Font: (Default) +Body (Arial), Font colour: Auto

Formatted: Font: (Default) +Body (Arial), Font colour: Auto

Deleted: The methodology to quantify vulnerability uses the equal weight analysis (EWA, e.g. Liu et al, (2020). Firstly, the individual indicators are standardized between 0 and 1, prior to aggregation (their sum); the standardization is done at the city level for all the years of record (1991, 2001, 2011) based on Equation 7: ¶
¶
$$\text{Standardized Indicator}\ (t) = \frac{\text{Indicator}(t) - \min(\text{Indicator}_{1991,2001,2011})}{\max(\text{Indicator}_{1991,2001,2011}) - \min\ (\text{Indicator}_{1991,2001,2011})}$$¶
(7)¶
Secondly, the EWA is performed according to Equation 8:¶
¶
$$\text{Vulnerability}\ (t) = \frac{\sum \text{Standardized indicator(t)}}{\text{number of indicators}}$$¶
(8)¶
This approach was chosen as it is the simplest method for weighing the vulnerability indicators and it is commonly applied in the literature with regards to HWs and CWs (e.g. Buscail et al., 2012; Buzási, 2022)The methodology to quantify vulnerability uses the equal weight analysis (EWA) with the indicators being standardized between 0 and 1 prior to aggregation according to Liu et al, (2020).

Formatted: Font: (Default) +Body (Arial), Font colour: Auto

Formatted: Font: (Default) +Body (Arial), Font colour: Auto, English (US)

Formatted: Font: (Default) +Body (Arial)

Formatted: Font: (Default) +Body (Arial)

Deleted: 10

Deleted: 6

Deleted: 6

Formatted: Font: (Default) +Body (Arial), Font colour: Auto

Deleted: Hazard is the probability of HWMId/CWMId derived from the Tweedie distribution

is therefore also bound by 0 and 1, with 0 corresponding to the lowest level of risk and 1 to the highest level of risk.

The risk is calculated at the municipality level because it is the lowest level of resolution of the three elements that compose it.

In order to further investigate which are the driving factors of the risk, we disentangle the marginal effect of each component (i.e. hazard, exposure, and vulnerability) for both HWs and CWs. In turn, one of them is allowed to vary across 1980-2018 and two of them are kept constant (to their value at the year 2003, the middle of the analyzed period).

3.6 Trends analysis & statistical significance

The trends are analyzed using the robust regression technique (Huber, 2011). This method is often used throughout the literature for natural hazards (Formetta and Feyen, 2019; Kishore et al., 2022).

The trends are analyzed using the robust regression technique (Huber, 2011). This method is often used throughout the literature for assessing trends in natural hazards (Formetta and Feyen, 2019 for multiple hazards and Kishore et al., 2022 specifically for HWs). To confirm the statistical significance of the trends the false discovery rate (FDR) methodology is used according to Wilks (2016) and Leung et al. (2019), with a significance level $\alpha=0.05$. The FDR is defined as the statistically expected fraction of null hypothesis test rejections at the grid cell for which the respective null hypotheses are actually true (Wilks 2016).

Deleted: Prior to standardization, we created yearly varying vulnerability maps for the period 1980-2018 using the vulnerability data available for the years 1991, 2001, 2011. This is performed using the same approach used for the population, meaning linear interpolation is used between 1991 and 2011 and the closest year was used for the periods of 1980-1990 and 2012-2018."¶ The yearly risk is calculated using both these standardized data (population and vulnerability) using equation 10.

Deleted: study

Deleted: the risk

Deleted: is also calculated and analyzed keeping on two of its three-component constant. This means, that three more analyses of the risks are done for both HWs and CWs, one with only the vulnerability changing, one keeping with only the exposure constant and one with only the hazard changing

Formatted: Font: (Default) +Body (Arial)

Formatted: Font: (Default) +Body (Arial)

Formatted: Font: (Default) +Body (Arial)

Formatted: Font: (Default) +Body (Arial), Font colour: Auto

Formatted: Space After: 7 pt, Border: Top: (No border), Bottom: (No border), Left: (No border), Right: (No border), Between : (No border)

Deleted:

Deleted:

Deleted: To confirm the significance of the trends and statistical tests throughout this article, the false discovery rate (FDR) methodology is used after (Wilks, 2016). The methodology is described in Leung et al, (2019), the desired significance level being set for the normal significance at $\alpha=0.05$, which after transformation to the significance for the FDR test becomes makes $\alpha_{FDR}=0.10$ for the false discover rate (Leung et al., 2019; Wilks, 2016). Leung et al, (2019) describes how to apply the methodology, readers are invited to consult this article (section 2.5) should they require more information on the application of the FDR significance test.

Formatted: Font:

4 Results

4.1 Hazard quantification and trends

For HWs hazard intensities, the most notable year on record (1980-2018) in the region is 2003, where HWMId reached a pixel maximum of 30.4 and a median value of 16.9 over the area (Figure S2 in the supplementary material). The second most intense HW occurred in 2015 and the third most intense in 1983. From the six years with the highest median HWMId between 1980 and 2018, four occurred in the last decade (2010, 2013, 2015, 2017), suggesting that climate change is already increasing the frequency of heat waves in the Trentino Alto-Adige region. For CW, only 1985 stands out, with a maximum and median CWMId of 27 and 14.5, respectively, or nearly three times more than that of any other year on record. The second strongest cold wave occurred in 2012.

A KS test (Figure S3 in the supplementary material) shows that the Tweedie distribution provides a good fit for both CWMId and HWMId, with power parameter values between [1,2] for the entire region. The KS goodness of fit test reveals a significance level of α_{sig}=5% as well as the false discovery rate for the significance level $2\alpha_{sig}$ for any pixel in the region. This permits us to estimate return levels for both HWs and CWs and analyze trends based on them. The return levels for return periods of 5 years (HW5Y, CW5Y) and 10 years (HW10Y, CW10Y) for every pixel are shown in Figure S4 in the supplementary material.

Fitting the robust linear model to the HWs values, statistically significant positive trends are found for HWs (i.e. HWMId > 0) and HWs with a magnitude larger than the 5-year event (HWMId > HW5Y) in most pixels of the region (Figure 2). For rarer events, those

Deleted: <#>On a temporal scale, the yearly risk calculation is done using the closest records of vulnerability and exposure to the year in question. This means, that for the 2003 HW risk, the 2003 HW hazard probabilities are combined with 2001 vulnerabilities (the closest census available year) and 2000 population (the closest population map available). The risk is calculated at city level because vulnerability is not available at a higher resolution. ¶

Deleted: <#> and discussions

Deleted: <#>¶

Deleted: <#>HW

Deleted: <#> –

Moved down [1]: <#> This aligns well with Russo et al. (2015), who have found very high HW in 1983, 2003 and 2015 in their analysis of the ten greatest HW in Europe since 1950

Deleted: <#>.

Moved down [2]: <#>This is in agreement with Jarzyna & Krzyżewska, (2021), who have found cold spells in those years (1985 and 2012) using different methodologies for other locations throughout Europe.

Deleted: –

Deleted: no rejection at a significance level of 5% for any pixel in the region

Deleted: HW

Deleted: CW

Deleted: T=

Deleted: T=

Deleted: –

Deleted: Using a Mann-Kendall trend test (Kendall, 1948)

Formatted: Font: (Default) +Body (Arial), Font colour: Auto

Formatted: Indent: Left: 0.14 cm, Don't keep with next, Border: Top: (No border), Bottom: (No border), Left: (No border), Right: (No border), Between : (No border), Tab stops: 0 cm, Left

Deleted: statistically significant positive trends are found for HW in most pixels of the region

Deleted: HW with a magnitude larger than the 5-year event (HWMId > HW5Y) also show a significant increasing trend over a large part of the region.

Formatted: Font: (Default) +Body (Arial), Font colour: Auto

Field Code Changed

larger than the 10-year event (HWMId > HW10Y), no statistically significant increase in HWs intensity are found in the region. With regards to the location of these trends, some of the highest parts of the regions have the greatest coefficient of increase (north of Bolzano and in the mountains located in the north-west of the region). For all CWs, we do not find statistically significant trends in any part of the region.

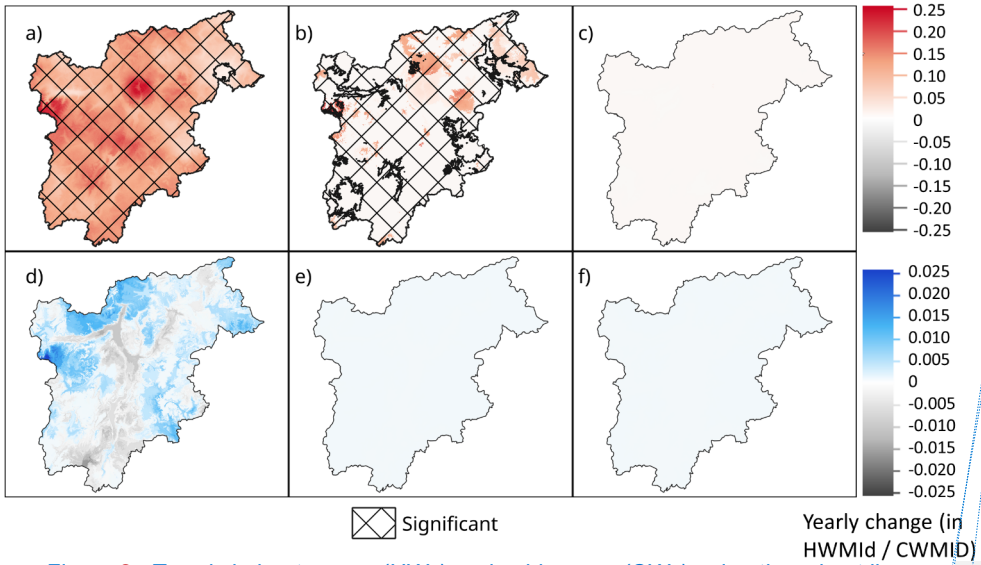

Figure 2: Trends in heat waves (HWs) and cold waves (CWs) using the robust linear model based on yearly HWMId and CWMId magnitudes from 1980 to 2018 for HWs a) with HWMId > 0, b) with HWMId > HW5Y, c) HWMId > HW10Y and for CWs and d) with CWMId > 0, e) with CWMId > CW5Y, f) CWMId > HW10Y.

Deleted: For rarer events; those larger than the 10-year event (HWMId > HW10Y), we find a statistically significant increase in HW intensity only in a portion of the region, mostly in upstream areas in the north but also around Bolzano

Deleted: In the three previous cases, for the rest of the region, the absence of statistical significance does not permit us to draw conclusions with regards to the trends. For CWs, we do not find statistically significant trends in any part of the region. The locations of presence / absence of these significant trends are further evidenced using the robust linear model ((Huber, 2011)) and previously used for HW by (Kishore et al., 2022)), see Figure S – 5 in the supplementary material.¶

Formatted: Font: Not Italic

Formatted: Caption, Line spacing: Double

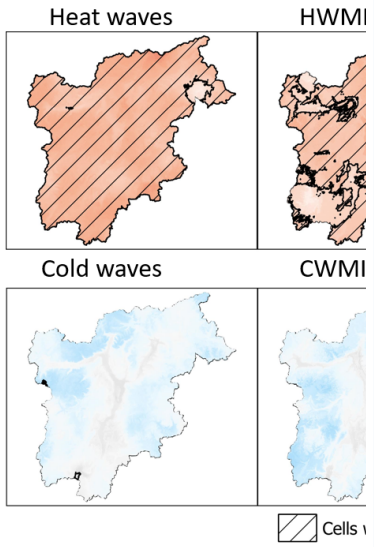

Deleted:
Figure 2: Trends in heat waves (HW) and cold waves (CW) using Mann-Kendall's test based on yearly HWMId and CWMId magnitudes from 1980 to 2018¶

4.2 Population exposure

In total, between 1980 and 2000, in the study region, about 900 000 people were exposed to a 5-year HW event, 250 000 to 10-year HW event, 3million to 5-year CW event and 1.9 million to 10-year CW event. Between 2000 and 2018, the values increased to over 5millions for 5-year HW event and to about 2.5million for 10-year HW event but decreased to 2.4 million for 5-year CW event and to 500 000 for 10-year CW event. However, due to the importance of the demographic change in the region (increase of population by 23%), it is important to study the percent of population impacted by these different events to understand whether these changes are due to demographic changes or the change in the frequency of events.

Figure 3 presents the share of the population exposed to HWs and CWs intensities larger than those of 5-year and 10-year events over the period 1980 to 2018 on a yearly basis. It shows that a higher share of the population was exposed to HWs more frequently after 2000 compared to the first two decades (80s and 90s). For both return periods, the robust linear model indicates a significant increase in population exposed to HWs over the region with a coefficient for the increase of nearly 1% per year for HWs>HW5Y and 0.02% for HWs>HW10Y. We did not find a significant trend in human exposure to CWs in the region.

Deleted: The significant increasing trend for HW that we find are consistent with literature that reported increasing HW trends in Europe over the last decades (Perkins-Kirkpatrick and Lewis, 2020; Piticar et al., 2018; Serrano-Notivoli et al., 2022; Spinoni et al., 2015; Zhang et al., 2020). The lack of trend in CW is also in agreement with previous research that could not detect any trend in extreme cold spells (Jarzyna and Krzyżewska, 2021; Piticar et al., 2018).¶

Formatted: Font: (Default) +Body (Arial)

Deleted: HW

Deleted: heatwave

Deleted: presents

Field Code Changed

Deleted: HW

Deleted: For both return periods, the Mann-Kendall test shows a significant increase in population exposed to HW over the region (Table T - 1 in the supplementary material). We did not find a trend in human exposure to CW in the region. Other statistical tests (Sen's slope and linear model) confirm these trends.

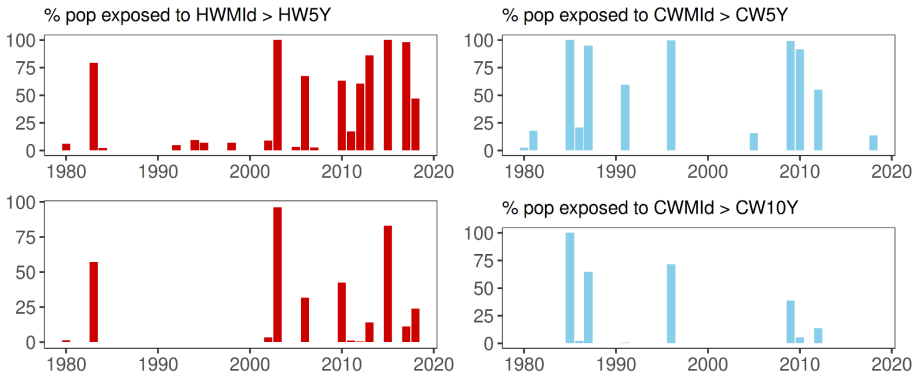

Figure 3: Percentage of population exposed to heat wave and cold wave events greater than the return levels of 5years and 10years over the span of 1980-2018

4.3 Vulnerability quantification

The vulnerability for the region (Figure 4: Calculated extreme temperatures vulnerability index for the three years of the census records (1991, 2001, 2011) with the borders of the municipalities in black) decreases in time, with an average value of 0.42 in 1991, 0.32 in 2001 and 0.27 in 2011. The main reason for the decrease in vulnerability at regional scale is the improvement in overall education level and housing conditions (i.e., fewer people living in old and poor housing conditions). However, by contrast, for the larger cities (those with a population over 30,000: Merano, Bolzano, Trento, Rovereto), the vulnerability has increased from 0.28 in 1991 to 0.30 in 2001 and 0.32 in 2011, averaged for those cities (see Figure S5 In the supplemental material). The increase in these cities' vulnerability relates to the older age indicator and social status, with a growing portion of the population above 55 and an increase in the number of isolated households (i.e., people living alone).

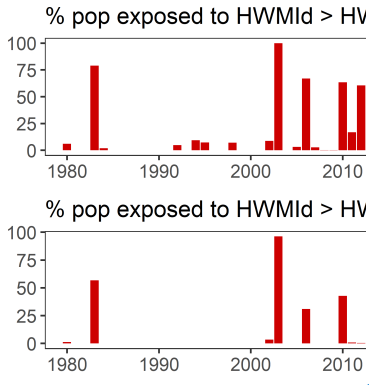

Deleted:

Formatted: Font: (Default) +Body (Arial)

Deleted: *Figure 3: Percentage of population exposed to heat wave and cold wave events*¶

Deleted: Figure 4Figure 4

Deleted: extreme

Moved down [3]: These two factors (elderly population and isolation) have also been found as some of the main factors for vulnerabilities in other regions of Europe (López-Bueno et al., 2021; Poumadère et al., 2005).

Deleted: The trends of increase and decrease in vulnerability found, however are not significant due to having only three data points. The uncertainty of these vulnerability findings and their trend are comparable to those of the census data they are extracted from.These two factors (elderly population and isolation) have also been found as some of the main factors for vulnerabilities in other regions of Europe (López-Bueno et al., 2021; Poumadère et al., 2005).

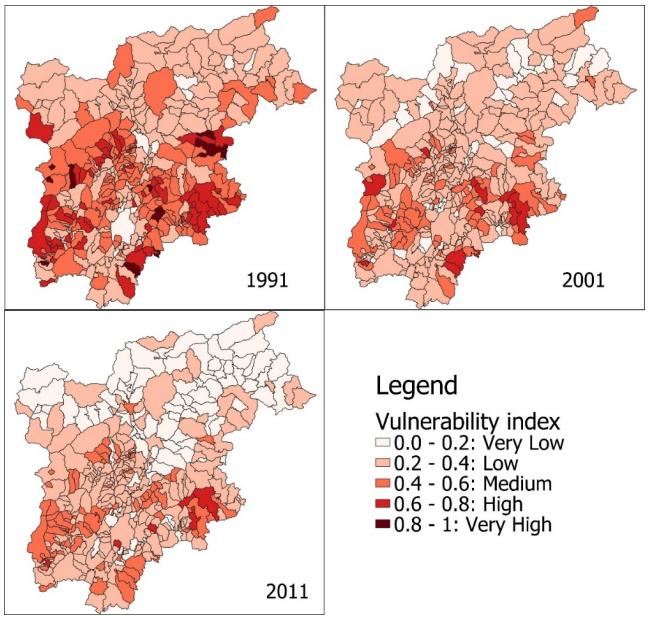

Figure 4: Calculated extreme temperatures vulnerability index for the three years of the census records (1991, 2001, 2011) with the borders of the municipalities in black.

4.4 Risk quantification

Figure 5 shows the trend in risk for the whole region over the period 1980-2018. The robust linear model shows significant increasing trend in HWs risk in 40% of the area, with a significant decreasing significant risk in some isolated parts of the region of study. While the risk from CWs has decreased over most of the region since the 1980s, in the major cities (Trento, Rovereto, Bolzano and Merano) we found an increase in CWs risk.

Formatted: Caption, Line spacing: Double

Deleted: *Figure 4: Calculated vulnerability index for the three years of the census records (1991, 2001, 2011)*¶

Deleted: The results of our vulnerability analysis somehow contrast with the findings of Frigerio & De Amicis (2016), who report increasing vulnerabilities for municipalities of the Bolzano province and slightly decreasing to steady vulnerabilities in the Trento province. This likely relates to the use of different indicators (employment, social-economic status, family structures, race/ethnicity, and population growth) and a different methodology for calculating the vulnerability. Notably in Frigerio & De Amicis (2016) the normalization of indicators is applied across all of Italy as opposed to only over the Trentino Alto-Adige region in this study, which may better characterize local vulnerability.¶

Formatted: Font: (Default) +Body (Arial)

Field Code Changed

Deleted: The Mann-Kendall test shows a significant increasing

Deleted: HW

Deleted: most

Deleted: CW

Deleted: ,

Deleted: CW

Deleted: The locations of presence/absence of these significant trends are further evidenced using the robust linear model (see Figure S – 6 in the supplementary material).

Decadal means of the annual regional risk values confirm these trend compart s, with the HWs risk increasing from 0.119 in the 1980s to 0.133 for the 2010s, while CWs risk has decreased from 0.134 in the 1980s to 0.124 in the 2010s. Decadal means of HWs risk for the large cities show a stronger trend compared to the whole region. We found that the average HWs risk in the main cities value increased by nearly a 45% increase in risk value compared to a 12% increase in the whole region. Decadal means of CWs risk for the main cities increased by nearly 17% increase whereas in the whole region, it decreased by 7%.

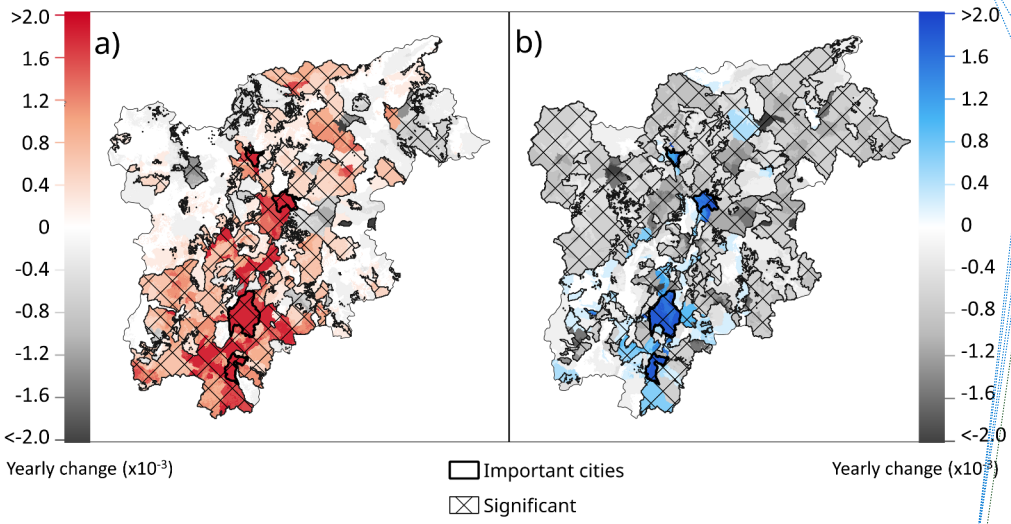

Figure 5: Trends of a) heat waves and b) cold waves risks using the robust linear method, colors indicating an increase in the risk and grey a decrease, significance is indicated with the hashing, the yearly change being the robust linear model coefficient.

Deleted: HW
Deleted: 113
Deleted: 126
Deleted: CW
Deleted: 26
Deleted: 17
Deleted: HW
Deleted: , w
Deleted: ith the
Deleted: large-city average
Deleted: ing from 0.263 to 0.386, or
Deleted: 0
Deleted: in HW risk for the
Deleted: CW
Deleted: big
Deleted: from 0.300 in the 1980s to 0.359 in the 2010s, or a
Deleted: 20
Deleted: increase
Moved down [5]: Similar finding are found with regards to the increase in HW risks by (Smid et al., 2019)), indicating an increase in the future for European capitals; however the same study highlights a future decrease in CW risk for these same cities. This is in contrast with the main cities of our study, where yet in the last four decades, CW risks are still found to be increasing. This could perhaps also be the case for other cities in mountainous regions such as highlighted by the case of Madrid in (López-Bueno et al., 2021) where its urban area was found to be the most at risk of CW as opposed to its rural area.
Deleted: in
Deleted: CW risk compared to a reduction of
Deleted: for the whole region
Deleted: .
Formatted: Font: (Default) +Body (Arial)
Formatted: Font: (Default) +Body (Arial)
Moved down [4]: This can be explained in part by the high population density in those cities, which is significantly larger than elsewhere in the region. Another factor is the increasing vulnerabilities in these cities relating to an increase in elderly and single households as previously mentioned
Deleted: It is further noted that the highest annual risk levels for both HW and CW coincide with the years with the highest hazard intensity (2003 for HW and 1985 for CW, see Figure S – 7 in the supplementary material), indicating that the hazard is the triggering factor f... [41]

The highest annual risk levels for both HWs and CWs coincide with the years with the highest hazard intensity (2003 for HW and 1985 for CW, see Figure S6 in the supplementary material), indicating that the hazard is potentially the main factor for risk. However, risks are further modulated by exposure and vulnerability. The risks are found to be the highest in the largest cities (Bolzano, Merano, Rovereto and Trento).

Figure 6 shows the marginal effect of the driving factor behind the trends in HWs and CWs risks. Figure 6-a, Figure 6-c, and Figure 6-e (Figure 6-b, Figure 6-d, and Figure 6-f) show the trend in HWs (CWs) risks with only vulnerability, only exposure, and only hazard changing, respectively.

The results in Figure 6-a and Figure 6-b show the same patterns as well as Figure 6-c and Figure 6-d because exposure and vulnerability are the same for both HWs and CWs and hazard is the only differing variable.

Figure 6-a (Figure 6-b) show increasing trends in risk (due to change in vulnerability only) in the main cities and nearby areas. Decreasing trends are found for most of the remaining region.

Figure 6-c (Figure 6-d) show increasing trends in risk (due to change in exposure only) in/near urban areas and decreasing trends in zones at high elevations and far from the urban centers.

Figure 6-d show that the hazard is the main driver of risk for HWs, with statistically significant increasing trends, more evident in and around highly populated areas. Finally, Figure 6-e show no significant trends in CWs risk (due to change in hazards only).

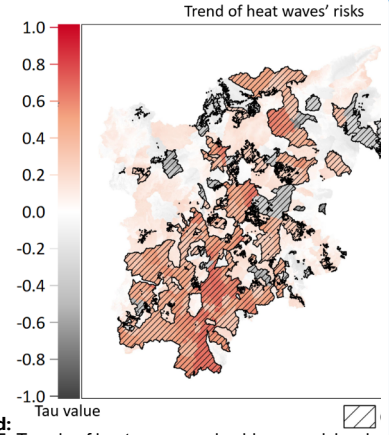

Deleted: Figure 5: Trends of heat waves and cold waves risks via the Mann-Kendall test.

Deleted: To find out precisely what were

Deleted: and the

Deleted: , the

Deleted: s

Deleted: are also computed with only a single variable changing

Deleted: for this can be seen

Deleted: 6. A)

Deleted: b)

Deleted: look the same

Deleted:

Deleted: c) and d), this is

Deleted: the only changing variable different in the

Deleted: risk is the Hazard

Deleted: .

Deleted: The trends with only the vulnerability changing shown in a) and b,

Deleted: significant trends throughout almost the entire region with them being negative for most of the region except for the large cities and their proximities where they are found to be positive

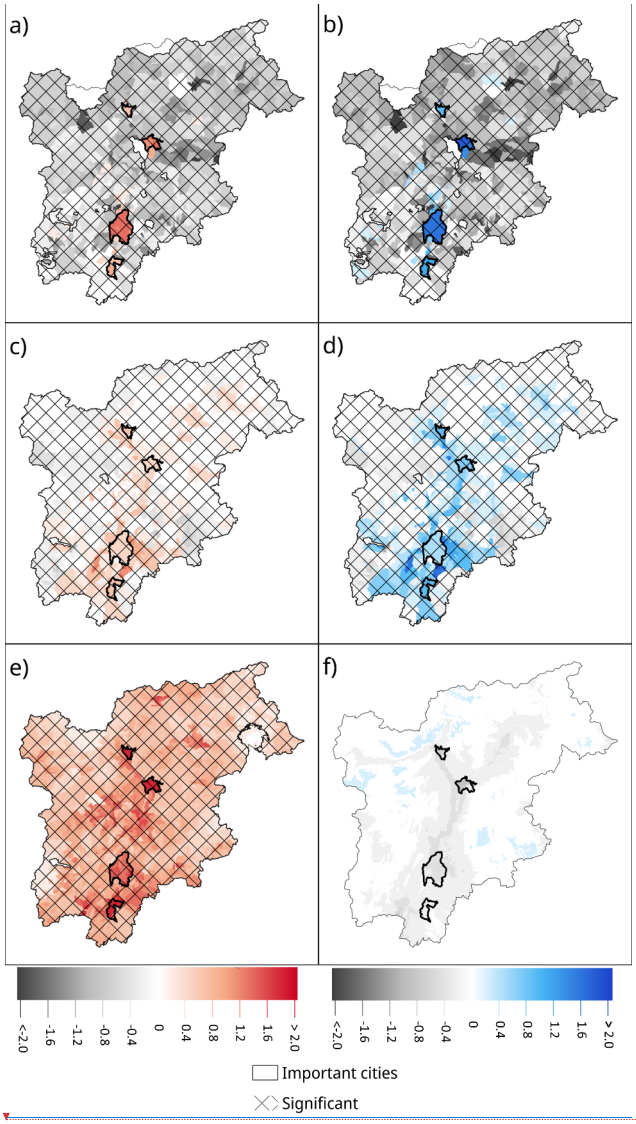

Figure 6: Trends of heat waves (and cold waves) risks due to changes in: a (b) vulnerability only, c (d) exposure only, and e (f) hazard only. Trends found with the

Deleted: The trends with only the population changing are shown in c) and d). The entire region shows significant trends with increasing trends in and near the urban areas and decreasing trends in the zone of higher elevations and further from the urban centers. The last two figures (e and f) show the change in risk through the hazard e) HWs and f) CWs. These trends show increasing trends for HWs and close to stagnant trends for CWs and those are only significant for most of the region for HWs.¶

Formatted: Font: (Default) +Body (Arial), Font colour: Auto

Formatted: Line spacing: Double

robust linear method, colors indicating an increase in the risk and grey a decrease, significance is indicated with the hashing, the yearly change being the robust linear model coefficient.

5 Discussion

The years found with the greatest HWs for the region agree with those of Russo et al. (2015), who found very high HWs in 1983, 2003 and 2015. The fact that four of the six largest HWs occurred in the last decade suggests that climate change is already influencing the intensity and frequency of HWs in the Trentino Alto-Adige region. With regards to CWs, Jarzyna & Krzyżewska, (2021), have also found cold spells in the years 1985 and 2012 using different methodologies for other locations throughout Europe. Similarly, other studies have also found the 1985 to be a year of an exceptional CW in Europe (Spinoni et al., 2015; Twardosz and Kossowska-Cezak, 2016).

The significant increasing trend we found in HWs events that we find are consistent with other studies in Europe over the last decades (e.g. Perkins-Kirkpatrick and Lewis, 2020; Piticar et al., 2018; Serrano-Notivoli et al., 2022; Spinoni et al., 2015; Zhang et al., 2020). The location of our highest increasing trends in HWs events are concordant to those of the higher increase in temperatures found at higher elevations by Acquaotta et al., (2015) in north-west Italy. Our results for HWs are also in line with the finding of Bacco et al., (2021) that analyzed trends in temperature extremes over northeastern regions of Italy (including Trentino Alto-Adige) based on homogenized data from dense station networks. They also found widespread warming, with significant positive trends in maximum-related mean and daytime temperature extremes. The lack of trend in CWs

Deleted: Figure 6: HWs and CWs risks trends coefficient of yearly change (x10^-3 colors indicating an increase in the risk and grey a decrease) and significance with only one changing variable and the two other constant: changing vulnerability a) HWs, b) CWs, changing exposure c) HWs d) CWs and changing hazard e) HWs f) CWs¶

Deleted: ¶
¶

Formatted: Font: (Default) +Body (Arial)

Formatted: Font: (Default) +Body (Arial)

Formatted: Font: (Default) +Body (Arial), Italian

Formatted: Font: (Default) +Body (Arial), Italian

Field Code Changed

Deleted: increase

Formatted: Italian

Deleted:

Deleted: (

Deleted:

Formatted: Font colour: Auto

events is also in agreement with previous research that could not detect any trend in extreme cold spells (Jarzyna and Krzyżewska, 2021; Piticar et al., 2018).

The trends in vulnerability and their absence of statical significance strongly depend on the available data. In our case they are the output of specific national census carried out every ten years and aggregated at the city spatial scale. From the other side, these data represent a freely available option to quantify the vulnerability to natural hazards, which is a crucial component for the risk quantification (e.g. Formetta and Feyen, 2019, Frigerio & De Amicis, 2016).

The two driving factors behind the increase in vulnerability (elderly population and isolation) have also been found as some of the main factors for vulnerabilities in other regions of Europe (López-Bueno et al., 2021; Poumadère et al., 2005). The results of our vulnerability analysis contrast with the findings of Frigerio & De Amicis (2016), who report increasing vulnerabilities for municipalities of the Bolzano province and slightly decreasing to steady vulnerabilities in the Trento province. This contrast, between our finding and theirs, is related to the use of different indicators (employment, social-economic status, family structures, race/ethnicity, and population growth) and a different methodology for calculating the vulnerability where the normalization of indicators is applied across all of Italy in their study, as opposed to only over the Trentino Alto-Adige region in this study, the latter characterizing better local vulnerability. The selection of different indicators and methodology might yield different results.

Our finding related to the increase in HWs risks are consistent with Smid et al., (2019), which showed indicates an increase in both current and the future period for European capitals; the same study highlights a future decrease in CWs risk for these same cities.

Formatted: Font: (Default) +Body (Arial)

Deleted: ¶

Formatted: Font: (Default) +Body (Arial), Font colour: Auto

Formatted: Font: (Default) +Body (Arial), Font colour: Auto

Formatted: Font: (Default) +Body (Arial), Font colour: Auto

Formatted: English (US), Pattern: Clear (White)

Formatted: Font: (Default) +Body (Arial)

Formatted: Font: (Default) +Body (Arial)

Formatted: Font: (Default) +Body (Arial)

We found that CWs risks is still increasing for the main cities of our study. This is also the case for other cities in mountainous regions such as highlighted by López-Bueno et al, (2021) for the city of Madrid, where its urban area was found to be the most at CWs risk compared to the rural area.

The analysis of the trends of risk while changing only one of its three variables and keeping constant the remaining two shows that hazard and vulnerability are the main driving factor of the HWs risk. The changes in HWs risk due to hazard also highlights the presence of urban heat island in the most populated cities of the region (in Figure 6-e these are the zones of the highest increasing trends in risk). This has also been found in other in urban areas (e.g. Morabito et al., 2021). The changes in CWs risk is mainly explained by the demographic and vulnerability changes, which are increasing in/around urban areas and decreasing elsewhere.

The changes found in HWs and CWs risk due to changes in exposure or vulnerability only is partially explained by rural-urban migration and an aging population, which is presented in other studies such as (Reynaud and Miccoli, 2018).

6 Summary and conclusions

Our study is one of the first to calculate risks of HWs and CWs and their trends at the community and city level for a region over 39 years. This is done by first quantifying the historical hazard of extreme temperature events using the HWMId and CWMId indicators, at high spatial resolution (250 m) in the Trentino Alto-Adige region for the period 1980-2018. The hazards probability of occurrences are then quantified by fitting a Tweedie distribution to the HWMId and CWMId values explicitly accounting directly for

Moved (insertion) [1]
Moved (insertion) [2]
Moved (insertion) [3]
Moved (insertion) [5]
Moved (insertion) [4]
Deleted: This aligns well with Russo et al. (2015), who have found very high HW in 1983, 2003 and 2015 in their analysis of the ten greatest HW in Europe since 1950This is in agreement with Jarzyna & Krzyżew ... [42]
Deleted: only
Deleted: permit
Deleted: us to draw the conclusion as to which ... [43]
Deleted: The changes in vulnerability previously ... [44]
Deleted: The demographic changes in the region ... [45]
Deleted: with
Deleted: only the hazard changing,
Deleted: in the case of HWs
Deleted: ,
Deleted: potential
Deleted: highlighted
Deleted: in Italy
Deleted: by
Deleted: (
Deleted:)
Deleted:
Deleted: Analyzing the risk with only a single cha ... [46]
Deleted: t
Deleted: changes
Deleted: are the contributing factors behind the tr ... [47]
Formatted ... [48]
Deleted: With regards to HWs, hazards and ... [49]
Formatted ... [50]
Deleted: HW
Deleted: CW
Deleted: mapping
Deleted: we mapped
Deleted: hazards
Deleted: sized
Deleted: using
Deleted: the novel method of
Deleted: while

zero values in their values time series. Two types of population exposure are found using the different hazard levels (5years and 10years return level). Vulnerability is calculated using 8 different socioeconomic indicators. Combining all these findings, the spatio-temporal HWs / CWs risk over the time period and at the city level is calculated.

Over the past 4 decades, HWs, i.e. HWMId>0, (and extreme HWs, i.e. HWMId>HW5Y) showed increasing trends in most of the region, with 98% (70%) being statistically significant. This results in an increasing exposure of people to extreme heat spells. For CW, we did not find a trend in hazard frequency and intensity and exposure to extreme cold remain constant. With regards to risks, in the region in general, a steady increase (~12%) in HWs risk and a decrease (~7%) in CWs risk are found. However, in the larger cities of the region, a much stronger rise in HWs risk (~45%) and CWs risk (~17%) occur. This is linked with demographic changes and the social status of city inhabitants, with more people and an ageing population living in cities and an increase in the number of people living alone.

The findings of this work shows that municipalities and cities in the Trentino Alto-Adige region have been seen increasing trends in HWs risk over the timeframe 1980-2018, while potentially experiencing the same levels of CWs risk. Our detailed analysis shows where to prioritize risk mitigation measures to reduce the hazard and vulnerability. Measures to mitigate heat in cities include, for example, greening of cities (Alsaad et al., 2022; Taleghani et al., 2019), while vulnerability could be decreased by improving the social and living conditions of citizens, especially of the elderly who are more vulnerable (Orlando et al., 2021; Poumadère et al., 2005; Vu et al., 2019), particularly in the cities of this region where they are becoming more numerous. If detailed data are available

Formatted: Font: (Default) +Body (Arial), Font colour: Auto
Deleted: Exposure is be found using the different fitted hazard levels
Formatted: Font: (Default) +Body (Arial), Font colour: Auto
Deleted: Using
Deleted: HW
Deleted: CW
Deleted:
Formatted ... [51]
Deleted: HWs had increasing trends in most of th ... [52]
Deleted: HW have occurred more frequently and ... [53]
Deleted: ,
Deleted: resulting
Deleted: a fairly constantconstant
Deleted: .
Deleted: . However, for these three points, vulner ... [54]
Deleted: In general, vulnerability is decreasing ov ... [55]
Deleted: , for smaller communitie
Deleted: but limited
Deleted: +
Deleted: 0
Deleted: HW
Deleted: -
Deleted: 9
Deleted: CW
Deleted: HW
Deleted: +
Deleted: 0
Deleted: an increase of around 20% in CW
Deleted: dwellers
Formatted ... [56]
Formatted ... [57]
Deleted: hazards
Formatted ... [58]
Deleted: hazards
Deleted: The findings of this work shows that ... [59]
Formatted ... [60]
Deleted:
Formatted ... [61]

for temperature, exposure and vulnerability indicators, the methodology presented here could be applied to other regions in- and outside Italy to help steer local climate adaptation investments at the city level.

Code availability

The code used for calculating HWMId and CWMId is free and open source, it is the extRemes package of R which is findable here: https://cran.r-project.org/package=extRemes.

Data availability

All data used in this study is available freely and openly online. The temperature data(Crespi et al., 2021) is available at the following location: https://doi.pangaea.de/10.1594/PANGAEA.924502. The population data from the GHSL is available at this location: https://data.jrc.ec.europa.eu/collection/ghsl. The indicator data used to calculate the vulnerable is available from ISTAT: https://www.istat.it/en/.

Formatted: Font: (Default) +Body (Arial), Bold
Formatted: Font: (Default) +Body (Arial)
Formatted: Font colour: Auto
Formatted: Font colour: Auto
Formatted: Font: (Default) +Body (Arial)
Formatted: Font: (Default) +Body (Arial)
Formatted: Font colour: Auto
Formatted: Font colour: Auto
Formatted: Font colour: Auto
Formatted: Font colour: Auto
Formatted: Font colour: Auto
Formatted: Font colour: Auto

References

Acquaotta, F., Fratianni, S., and Garzena, D.: Temperature changes in the North-Western Italian Alps from 1961 to 2010, Theor. Appl. Climatol., 122, 619–634, https://doi.org/10.1007/s00704-014-1316-7, 2015.

Alsaad, H., Hartmann, M., Hilbel, R., and Voelker, C.: The potential of facade greening in mitigating the effects of heatwaves in Central European cities, Build. Environ., 216, 109021, https://doi.org/10.1016/j.buildenv.2022.109021, 2022.

Bacco, M. D. and Scorzini, A. R.: Recent changes in temperature extremes across the north-eastern region of Italy and their relationship with large-scale circulation, Clim. Res., 81, 167–185, https://doi.org/10.3354/cr01614, 2020.

Bonat, W. H. and Kokonendji, C. C.: Flexible Tweedie regression models for continuous data, J. Stat. Comput. Simul., 87, 2138–2152, https://doi.org/10.1080/00949655.2017.1318876, 2017.

Buscail, C., Upegui, E., and Viel, J.-F.: Mapping heatwave health risk at the community level for public health action, Int. J. Health Geogr., 11, 38, https://doi.org/10.1186/1476-072X-11-38, 2012.

Buzási, A.: Comparative assessment of heatwave vulnerability factors for the districts of Budapest, Hungary, Urban Clim., 42, 101127, https://doi.org/10.1016/j.uclim.2022.101127, 2022.

Ceccherini, G., Russo, S., Ameztoy, I., Marchese, A. F., and Carmona-Moreno, C.: Heat waves in Africa 1981–2015, observations and reanalysis, Nat. Hazards Earth Syst. Sci., 17, 115–125, https://doi.org/10.5194/nhess-17-115-2017, 2017.

Chambers, J.: Global and cross-country analysis of exposure of vulnerable populations to heatwaves from 1980 to 2018, Clim. Change, 163, 539–558, https://doi.org/10.1007/s10584-020-02884-2, 2020.

Cheng, W., Li, D., Liu, Z., and Brown, R. D.: Approaches for identifying heat-vulnerable populations and locations: A systematic review, Sci. Total Environ., 799, 149417, https://doi.org/10.1016/j.scitotenv.2021.149417, 2021.

Conti, S., Meli, P., Minelli, G., Solimini, R., Toccaceli, V., Vichi, M., Beltrano, C., and Perini, L.: Epidemiologic study of mortality during the Summer 2003 heat wave in Italy, Environ. Res., 98, 390–399, https://doi.org/10.1016/j.envres.2004.10.009, 2005.

Crespi, A., Matiu, M., Bertoldi, G., Petitta, M., and Zebisch, M.: A high-resolution gridded dataset of daily temperature and precipitation records (1980–2018) for Trentino – South Tyrol (north-eastern Italian Alps), Earth Syst. Sci. Data Discuss., 1–27, https://doi.org/10.5194/essd-2020-346, 2021.

de'Donato, F. K., Leone, M., Noce, D., Davoli, M., and Michelozzi, P.: The Impact of the February 2012 Cold Spell on Health in Italy Using Surveillance Data, PLOS ONE, 8, e61720, https://doi.org/10.1371/journal.pone.0061720, 2013.

Dong, J., Peng, J., He, X., Corcoran, J., Qiu, S., and Wang, X.: Heatwave-induced human health risk assessment in megacities based on heat stress-social vulnerability-

human exposure framework, Landsc. Urban Plan., 203, 103907, https://doi.org/10.1016/j.landurbplan.2020.103907, 2020.

Dosio, A., Mentaschi, L., Fischer, E. M., and Wyser, K.: Extreme heat waves under 1.5\hspace0.167em°C and 2\hspace0.167em°C global warming, Environ. Res. Lett., 13, 054006, https://doi.org/10.1088/1748-9326/aab827, 2018.

Dunn, P. K.: Occurrence and quantity of precipitation can be modelled simultaneously, Int. J. Climatol., 24, 1231–1239, https://doi.org/10.1002/joc.1063, 2004.

Dunn, P. K.: tweedie: Evaluation of Tweedie Exponential Family Models, 2021.

Ellena, M., Ballester, J., Mercogliano, P., Ferracin, E., Barbato, G., Costa, G., and Ingole, V.: Social inequalities in heat-attributable mortality in the city of Turin, northwest of Italy: a time series analysis from 1982 to 2018, Environ. Health, 19, 116, https://doi.org/10.1186/s12940-020-00667-x, 2020.

El-Zein, A. and Tonmoy, F. N.: Assessment of vulnerability to climate change using a multi-criteria outranking approach with application to heat stress in Sydney, Ecol. Indic., 48, 207–217, https://doi.org/10.1016/j.ecolind.2014.08.012, 2015.

Estoque, R. C., Ooba, M., Seposo, X. T., Togawa, T., Hijioka, Y., Takahashi, K., and Nakamura, S.: Heat health risk assessment in Philippine cities using remotely sensed data and social-ecological indicators, Nat. Commun., 11, 1581, https://doi.org/10.1038/s41467-020-15218-8, 2020.

Formetta, G. and Feyen, L.: Empirical evidence of declining global vulnerability to climate-related hazards, Glob. Environ. Change, 57, 101920, https://doi.org/10.1016/j.gloenvcha.2019.05.004, 2019.

Fratianni, S. and Acquaotta, F.: The Climate of Italy, in: Landscapes and Landforms of Italy, edited by: Soldati, M. and Marchetti, M., Springer International Publishing, Cham, 29–38, https://doi.org/10.1007/978-3-319-26194-2_4, 2017.

Frigerio, I. and De Amicis, M.: Mapping social vulnerability to natural hazards in Italy: A suitable tool for risk mitigation strategies, Environ. Sci. Policy, 63, 187–196, https://doi.org/10.1016/j.envsci.2016.06.001, 2016.

García-León, D., Casanueva, A., Standardi, G., Burgstall, A., Flouris, A. D., and Nybo, L.: Current and projected regional economic impacts of heatwaves in Europe, Nat. Commun., 12, 5807, https://doi.org/10.1038/s41467-021-26050-z, 2021.

Gasparrini, A., Guo, Y., Hashizume, M., Lavigne, E., Zanobetti, A., Schwartz, J., Tobias, A., Tong, S., Rocklöv, J., Forsberg, B., Leone, M., Sario, M. D., Bell, M. L., Guo, Y.-L. L., Wu, C., Kan, H., Yi, S.-M., Coelho, M. de S. Z. S., Saldiva, P. H. N., Honda, Y., Kim, H., and Armstrong, B.: Mortality risk attributable to high and low ambient temperature: a multicountry observational study, The Lancet, 386, 369–375, https://doi.org/10.1016/S0140-6736(14)62114-0, 2015.

Goffard, P.-O., Jammalamadaka, S. R., and Meintanis, S.: Goodness-of-fit tests for compound distributions with applications in insurance, 2019.

Habeeb, D., Vargo, J., and Stone, B.: Rising heat wave trends in large US cities, Nat. Hazards, 76, 1651–1665, https://doi.org/10.1007/s11069-014-1563-z, 2015.

Hasan, M. M. and Dunn, P. K.: Two Tweedie distributions that are near-optimal for modelling monthly rainfall in Australia, Int. J. Climatol., 31, 1389–1397, https://doi.org/10.1002/joc.2162, 2011.

Ho, H. C., Knudby, A., Chi, G., Aminipouri, M., and Lai, D. Y.-F.: Spatiotemporal analysis of regional socio-economic vulnerability change associated with heat risks in Canada, Appl. Geogr., 95, 61–70, https://doi.org/10.1016/j.apgeog.2018.04.015, 2018.

Huber, P. J.: Robust Statistics, in: International Encyclopedia of Statistical Science, edited by: Lovric, M., Springer, Berlin, Heidelberg, 1248–1251, https://doi.org/10.1007/978-3-642-04898-2_594, 2011.

IPCC: Climate Change 2014 – Impacts, Adaptation and Vulnerability: Part A: Global and Sectoral Aspects: Working Group II Contribution to the IPCC Fifth Assessment Report: Volume 1: Global and Sectoral Aspects, Cambridge University Press, Cambridge, https://doi.org/10.1017/CBO9781107415379, 2014.

Istat.it - 15° Censimento della popolazione e delle abitazioni 2011: https://www.istat.it/it/censimenti-permanenti/censimenti-precedenti/popolazione-e-abitazioni/popolazione-2011, last access: 16 November 2021.

Jarzyna, K. and Krzyżewska, A.: Cold spell variability in Europe in relation to the degree of climate continentalism in 1981–2018 period, Weather, 76, 122–128, https://doi.org/10.1002/wea.3937, 2021.

Johnson, W. D., Burton, J. H., Beyl, R. A., and Romer, J. E.: A Simple Chi-Square Statistic for Testing Homogeneity of Zero-Inflated Distributions, Open J. Stat., 5, 483, https://doi.org/10.4236/ojs.2015.56050, 2015.

Jorgensen, B.: Exponential Dispersion Models, J. R. Stat. Soc. Ser. B Methodol., 49, 127–162, 1987.

Karanja, J. and Kiage, L.: Perspectives on spatial representation of urban heat vulnerability, Sci. Total Environ., 774, 145634, https://doi.org/10.1016/j.scitotenv.2021.145634, 2021.

Kim, D.-W., Deo, R. C., Lee, J.-S., and Yeom, J.-M.: Mapping heatwave vulnerability in Korea, Nat. Hazards, 89, 35–55, https://doi.org/10.1007/s11069-017-2951-y, 2017.

King, A. D., Donat, M. G., Lewis, S. C., Henley, B. J., Mitchell, D. M., Stott, P. A., Fischer, E. M., and Karoly, D. J.: Reduced heat exposure by limiting global warming to 1.5 °C, Nat. Clim. Change, 8, 549–551, https://doi.org/10.1038/s41558-018-0191-0, 2018.

Kishore, P., Basha, G., Venkat Ratnam, M., AghaKouchak, A., Sun, Q., Velicogna, I., and Ouarda, T. B. J. M.: Anthropogenic influence on the changing risk of heat waves over India, Sci. Rep., 12, 3337, https://doi.org/10.1038/s41598-022-07373-3, 2022.

Kron, W., Löw, P., and Kundzewicz, Z. W.: Changes in risk of extreme weather events in Europe, Environ. Sci. Policy, 100, 74–83, https://doi.org/10.1016/j.envsci.2019.06.007, 2019.

Liu, X., Yue, W., Yang, X., Hu, K., Zhang, W., and Huang, M.: Mapping Urban Heat Vulnerability of Extreme Heat in Hangzhou via Comparing Two Approaches, Complexity, 2020, e9717658, https://doi.org/10.1155/2020/9717658, 2020.

López-Bueno, J. A., Navas-Martín, M. Á., Díaz, J., Mirón, I. J., Luna, M. Y., Sánchez-Martínez, G., Culqui, D., and Linares, C.: The effect of cold waves on mortality in urban and rural areas of Madrid, Environ. Sci. Eur., 33, 72, https://doi.org/10.1186/s12302-021-00512-z, 2021.

Michelozzi, P., de 'Donato, F., Bisanti, L., Russo, A., Cadum, E., DeMaria, M., D'Ovidio, M., Costa, G., and Perucci, C. A.: Heat Waves in Italy: Cause Specific Mortality and the Role of Educational Level and Socio-Economic Conditions, in: Extreme Weather Events and Public Health Responses, edited by: Kirch, W., Bertollini, R., and Menne, B., Springer, Berlin, Heidelberg, 121–127, https://doi.org/10.1007/3-540-28862-7_12, 2005.

Michelozzi, P., De' Donato, F., Scortichini, M., De Sario, M., Asta, F., Agabiti, N., Guerra, R., de Martino, A., and Davoli, M.: [On the increase in mortality in Italy in 2015: analysis of seasonal mortality in the 32 municipalities included in the Surveillance system of daily mortality], Epidemiol. Prev., 40, 22–28, https://doi.org/10.19191/EP16.1.P022.010, 2016.

Morabito, M., Crisci, A., Gioli, B., Gualtieri, G., Toscano, P., Stefano, V. D., Orlandini, S., and Gensini, G. F.: Urban-Hazard Risk Analysis: Mapping of Heat-Related Risks in the Elderly in Major Italian Cities, PLOS ONE, 10, e0127277, https://doi.org/10.1371/journal.pone.0127277, 2015.

Morabito, M., Crisci, A., Guerri, G., Messeri, A., Congedo, L., and Munafò, M.: Surface urban heat islands in Italian metropolitan cities: Tree cover and impervious surface influences, Sci. Total Environ., 751, 142334, https://doi.org/10.1016/j.scitotenv.2020.142334, 2021.

Neumayer, E. and Barthel, F.: Normalizing economic loss from natural disasters: A global analysis, Glob. Environ. Change, 21, 13–24, https://doi.org/10.1016/j.gloenvcha.2010.10.004, 2011.

Oldenborgh, G. J. van, Mitchell-Larson, E., Vecchi, G. A., Vries, H. de, Vautard, R., and Otto, F.: Cold waves are getting milder in the northern midlatitudes, Environ. Res. Lett., 14, 114004, https://doi.org/10.1088/1748-9326/ab4867, 2019.

Orlando, S., Mosconi, C., De Santo, C., Emberti Gialloreti, L., Inzerilli, M. C., Madaro, O., Mancinelli, S., Ciccacci, F., Marazzi, M. C., Palombi, L., and Liotta, G.: The Effectiveness of Intervening on Social Isolation to Reduce Mortality during Heat Waves in Aged Population: A Retrospective Ecological Study, Int. J. Environ. Res. Public. Health, 18, 11587, https://doi.org/10.3390/ijerph182111587, 2021.

Papathoma-Köhle, M., Ulbrich, T., Keiler, M., Pedoth, L., Totschnig, R., Glade, T., Schneiderbauer, S., and Eidswig, U.: Chapter 8 - Vulnerability to Heat Waves, Floods, and Landslides in Mountainous Terrain: Test Cases in South Tyrol, in: Assessment of Vulnerability to Natural Hazards, edited by: Birkmann, J., Kienberger, S., and Alexander, D. E., Elsevier, 179–201, https://doi.org/10.1016/B978-0-12-410528-7.00008-4, 2014.

Peng, J., Liu, Y., Li, T., and Wu, J.: Regional ecosystem health response to rural land use change: A case study in Lijiang City, China, Ecol. Indic., 72, 399–410, https://doi.org/10.1016/j.ecolind.2016.08.024, 2017.

Perkins-Kirkpatrick, S. E. and Gibson, P. B.: Changes in regional heatwave characteristics as a function of increasing global temperature, Sci. Rep., 7, 12256, https://doi.org/10.1038/s41598-017-12520-2, 2017.

Perkins-Kirkpatrick, S. E. and Lewis, S. C.: Increasing trends in regional heatwaves, Nat. Commun., 11, 3357, https://doi.org/10.1038/s41467-020-16970-7, 2020.

Piticar, A., Croitoru, A.-E., Ciupertea, F.-A., and Harpa, G.-V.: Recent changes in heat waves and cold waves detected based on excess heat factor and excess cold factor in Romania, Int. J. Climatol., 38, 1777–1793, https://doi.org/10.1002/joc.5295, 2018.

Poumadère, M., Mays, C., Le Mer, S., and Blong, R.: The 2003 Heat Wave in France: Dangerous Climate Change Here and Now, Risk Anal., 25, 1483–1494, https://doi.org/10.1111/j.1539-6924.2005.00694.x, 2005.

Quader, M. A., Khan, A. U., and Kervyn, M.: Assessing Risks from Cyclones for Human Lives and Livelihoods in the Coastal Region of Bangladesh, Int. J. Environ. Res. Public. Health, 14, E831, https://doi.org/10.3390/ijerph14080831, 2017.

Rahma, A. and Kokonendji, C. C.: Discriminating between and within (semi)continuous classes of both Tweedie and geometric Tweedie models, J. Stat. Comput. Simul., 2021.

Reid, C. E., O'Neill Marie S., Gronlund Carina J., Brines Shannon J., Brown Daniel G., Diez-Roux Ana V., and Schwartz Joel: Mapping Community Determinants of Heat Vulnerability, Environ. Health Perspect., 117, 1730–1736, https://doi.org/10.1289/ehp.0900683, 2009.

Reynaud, C. and Miccoli, S.: Depopulation and the Aging Population: The Relationship in Italian Municipalities, Sustainability, 10, 1004, https://doi.org/10.3390/su10041004, 2018.

Russo, S., Sillmann, J., and Fischer, E. M.: Top ten European heatwaves since 1950 and their occurrence in the coming decades, Environ. Res. Lett., 10, 124003, https://doi.org/10.1088/1748-9326/10/12/124003, 2015.

Russo, S., Marchese, A. F., Sillmann, J., and Immé, G.: When will unusual heat waves become normal in a warming Africa?, Environ. Res. Lett., 11, 054016, https://doi.org/10.1088/1748-9326/11/5/054016, 2016.

Russo, S., Sillmann, J., Sippel, S., Barcikowska, M. J., Ghisetti, C., Smid, M., and O'Neill, B.: Half a degree and rapid socioeconomic development matter for heatwave risk, Nat. Commun., 10, 136, https://doi.org/10.1038/s41467-018-08070-4, 2019.

Schiavina, M., Freire, S., and MacManus, K.: GHS-POP R2019A - GHS population grid multitemporal (1975-1990-2000-2015), https://doi.org/10.2905/0C6B9751-A71F-4062-830B-43C9F432370F, 2019.

Serrano-Notivoli, R., Lemus-Canovas, M., Barrao, S., Sarricolea, P., Meseguer-Ruiz, O., and Tejedor, E.: Heat and cold waves in mainland Spain: Origins, characteristics,

and trends, Weather Clim. Extrem., 37, 100471, https://doi.org/10.1016/j.wace.2022.100471, 2022.

Shono, H.: Application of the Tweedie distribution to zero-catch data in CPUE analysis, Fish. Res., 93, 154–162, https://doi.org/10.1016/j.fishres.2008.03.006, 2008.

Smid, M., Russo, S., Costa, A. C., Granell, C., and Pebesma, E.: Ranking European capitals by exposure to heat waves and cold waves, Urban Clim., 27, 388–402, https://doi.org/10.1016/j.uclim.2018.12.010, 2019.

Spinoni, J., Lakatos, M., Szentimrey, T., Bihari, Z., Szalai, S., Vogt, J., and Antofie, T.: Heat and cold waves trends in the Carpathian Region from 1961 to 2010, Int. J. Climatol., 35, 4197–4209, https://doi.org/10.1002/joc.4279, 2015.

Taleghani, M., Marshall, A., Fitton, R., and Swan, W.: Renaturing a microclimate: The impact of greening a neighbourhood on indoor thermal comfort during a heatwave in Manchester, UK, Sol. Energy, 182, 245–255, https://doi.org/10.1016/j.solener.2019.02.062, 2019.

Temple, S. D.: The Tweedie Index Parameter and Its Estimator An Introduction with Applications to Actuarial Ratemaking, 2018.

Tijdeman, E., Stahl, K., and Tallaksen, L. M.: Drought Characteristics Derived Based on the Standardized Streamflow Index: A Large Sample Comparison for Parametric and Nonparametric Methods, Water Resour. Res., 56, https://doi.org/10.1029/2019WR026315, 2020.

Tuholske, C., Caylor, K., Funk, C., Verdin, A., Sweeney, S., Grace, K., Peterson, P., and Evans, T.: Global urban population exposure to extreme heat, Proc. Natl. Acad. Sci., 118, e2024792118, https://doi.org/10.1073/pnas.2024792118, 2021.

Twardosz, R. and Kossowska-Cezak, U.: Exceptionally cold and mild winters in Europe (1951–2010), Theor. Appl. Climatol., 125, 399–411, https://doi.org/10.1007/s00704-015-1524-9, 2016.

Tweedie, M. C. K.: An index which distinguishes between some important exponential families, in: Statistics: applications and new directions (Calcutta, 1981), Indian Statist. Inst., Calcutta, 579–604, 1984.

Disaster risk: https://www.undrr.org/terminology/disaster-risk, last access: 21 November 2021.

Vu, A., Rutherford, S., and Phung, D.: Heat Health Prevention Measures and Adaptation in Older Populations—A Systematic Review, Int. J. Environ. Res. Public. Health, 16, 4370, https://doi.org/10.3390/ijerph16224370, 2019.

Watts, N., Amann, M., Arnell, N., Ayeb-Karlsson, S., Belesova, K., Berry, H., Bouley, T., Boykoff, M., Byass, P., Cai, W., Campbell-Lendrum, D., Chambers, J., Daly, M., Dasandi, N., Davies, M., Depoux, A., Dominguez-Salas, P., Drummond, P., Ebi, K. L., Ekins, P., Montoya, L. F., Fischer, H., Georgeson, L., Grace, D., Graham, H., Hamilton, I., Hartinger, S., Hess, J., Kelman, I., Kiesewetter, G., Kjellstrom, T., Kniveton, D., Lemke, B., Liang, L., Lott, M., Lowe, R., Sewe, M. O., Martinez-Urtaza, J., Maslin, M., McAllister, L., Mikhaylov, S. J., Milner, J., Moradi-Lakeh, M., Morrissey, K., Murray, K.,

Nilsson, M., Neville, T., Oreszczyn, T., Owfi, F., Pearman, O., Pencheon, D., Pye, S., Rabbaniha, M., Robinson, E., Rocklöv, J., Saxer, O., Schütte, S., Semenza, J. C., Shumake-Guillemot, J., Steinbach, R., Tabatabaei, M., Tomei, J., Trinanes, J., Wheeler, N., Wilkinson, P., Gong, P., Montgomery, H., and Costello, A.: The 2018 report of the Lancet Countdown on health and climate change: shaping the health of nations for centuries to come, The Lancet, 392, 2479–2514, https://doi.org/10.1016/S0140-6736(18)32594-7, 2018.

Zhang, R., Sun, C., Zhu, J., Zhang, R., and Li, W.: Increased European heat waves in recent decades in response to shrinking Arctic sea ice and Eurasian snow cover, Npj Clim. Atmospheric Sci., 3, 1–9, https://doi.org/10.1038/s41612-020-0110-8, 2020.

Page 1: [1] Formatted Formetta Giuseppe 19/02/2023 10:23:00

Not Highlight

Page 1: [1] Formatted Formetta Giuseppe 19/02/2023 10:23:00

Not Highlight

Page 1: [2] Deleted Morlot, Martin Jean-luc Emile 13/01/2023 11:10:00

Page 1: [2] Deleted Morlot, Martin Jean-luc Emile 13/01/2023 11:10:00

Page 1: [2] Deleted Morlot, Martin Jean-luc Emile 13/01/2023 11:10:00

Page 1: [2] Deleted Morlot, Martin Jean-luc Emile 13/01/2023 11:10:00

Page 1: [3] Deleted Formetta Giuseppe 19/02/2023 11:57:00

Page 1: [3] Deleted Formetta Giuseppe 19/02/2023 11:57:00

Page 1: [4] Deleted Formetta Giuseppe 19/02/2023 11:58:00

Page 1: [4] Deleted Formetta Giuseppe 19/02/2023 11:58:00

Page 1: [4] Deleted Formetta Giuseppe 19/02/2023 11:58:00

Page 1: [4] Deleted Formetta Giuseppe 19/02/2023 11:58:00

Page 1: [5] Deleted Morlot, Martin Jean-luc Emile 13/01/2023 10:34:00

Page 1: [5] Deleted Morlot, Martin Jean-luc Emile 13/01/2023 10:34:00

Page 1: [6] Deleted Morlot, Martin Jean-luc Emile 13/01/2023 11:10:00

Page 1: [6] Deleted Morlot, Martin Jean-luc Emile 13/01/2023 11:10:00

Page 1: [7] Deleted Formetta Giuseppe 19/02/2023 12:01:00

Page 1: [7] Deleted Formetta Giuseppe 19/02/2023 12:01:00

Page 2: [8] Deleted Martin Morlot 19/02/2023 12:33:00

Page 2: [8] Deleted Martin Morlot 19/02/2023 12:33:00

Page 2: [9] Deleted Morlot, Martin Jean-luc Emile 13/01/2023 11:01:00

Page 2: [9] Deleted Morlot, Martin Jean-luc Emile 13/01/2023 11:01:00

Page 2: [9] Deleted Morlot, Martin Jean-luc Emile 13/01/2023 11:01:00

Page 2: [9] Deleted Morlot, Martin Jean-luc Emile 13/01/2023 11:01:00

Page 2: [9] Deleted Morlot, Martin Jean-luc Emile 13/01/2023 11:01:00

Page 2: [9] Deleted Morlot, Martin Jean-luc Emile 13/01/2023 11:01:00

Page 2: [9] Deleted Morlot, Martin Jean-luc Emile 13/01/2023 11:01:00

Page 2: [9] Deleted Morlot, Martin Jean-luc Emile 13/01/2023 11:01:00

Page 2: [10] Deleted Morlot, Martin Jean-luc Emile 13/01/2023 11:05:00

Page 2: [10] Deleted Morlot, Martin Jean-luc Emile 13/01/2023 11:05:00

Page 2: [10] Deleted Morlot, Martin Jean-luc Emile 13/01/2023 11:05:00

Page 2: [10] Deleted Morlot, Martin Jean-luc Emile 13/01/2023 11:05:00

Page 2: [10] Deleted Morlot, Martin Jean-luc Emile 13/01/2023 11:05:00

Page 2: [10] Deleted Morlot, Martin Jean-luc Emile 13/01/2023 11:05:00

Page 2: [10] Deleted **Morlot, Martin Jean-luc Emile** **13/01/2023 11:05:00**

Page 2: [11] Deleted **Morlot, Martin Jean-luc Emile** **13/01/2023 10:35:00**

Page 2: [11] Deleted **Morlot, Martin Jean-luc Emile** **13/01/2023 10:35:00**

Page 2: [11] Deleted **Morlot, Martin Jean-luc Emile** **13/01/2023 10:35:00**

Page 2: [11] Deleted **Morlot, Martin Jean-luc Emile** **13/01/2023 10:35:00**

Page 2: [11] Deleted **Morlot, Martin Jean-luc Emile** **13/01/2023 10:35:00**

Page 2: [12] Deleted **Morlot, Martin Jean-luc Emile** **19/01/2023 13:31:00**

Page 2: [12] Deleted **Morlot, Martin Jean-luc Emile** **19/01/2023 13:31:00**

Page 2: [12] Deleted **Morlot, Martin Jean-luc Emile** **19/01/2023 13:31:00**

Page 2: [13] Formatted **Formetta Giuseppe** **19/02/2023 10:23:00**

Not Highlight

Page 2: [13] Formatted **Formetta Giuseppe** **19/02/2023 10:23:00**

Not Highlight

Page 2: [14] Deleted **Morlot, Martin Jean-luc Emile** **13/01/2023 11:33:00**

Page 2: [14] Deleted Morlot, Martin Jean-luc Emile 13/01/2023 11:33:00

Page 2: [15] Deleted Morlot, Martin Jean-luc Emile 13/01/2023 11:32:00

Page 2: [15] Deleted Morlot, Martin Jean-luc Emile 13/01/2023 11:32:00

Page 2: [16] Formatted Formetta Giuseppe 19/02/2023 10:23:00

Italian

Page 2: [16] Formatted Formetta Giuseppe 19/02/2023 10:23:00

Italian

Page 2: [17] Deleted Morlot, Martin Jean-luc Emile 19/01/2023 13:39:00

Page 2: [17] Deleted Morlot, Martin Jean-luc Emile 19/01/2023 13:39:00

Page 2: [17] Deleted Morlot, Martin Jean-luc Emile 19/01/2023 13:39:00

Page 2: [17] Deleted Morlot, Martin Jean-luc Emile 19/01/2023 13:39:00

Page 2: [17] Deleted Morlot, Martin Jean-luc Emile 19/01/2023 13:39:00

Page 2: [18] Deleted Formetta Giuseppe 19/02/2023 10:26:00

Page 2: [19] Deleted Morlot, Martin Jean-luc Emile 19/01/2023 13:32:00

Page 2: [19] Deleted Morlot, Martin Jean-luc Emile 19/01/2023 13:32:00

Page 2: [19] Deleted Morlot, Martin Jean-luc Emile 19/01/2023 13:32:00

Page 4: [20] Deleted Formetta Giuseppe 19/02/2023 10:31:00

Page 4: [20] Deleted Formetta Giuseppe 19/02/2023 10:31:00

Page 4: [21] Deleted Formetta Giuseppe 19/02/2023 10:31:00

Page 4: [21] Deleted Formetta Giuseppe 19/02/2023 10:31:00

Page 4: [22] Deleted Martin Morlot 19/02/2023 09:30:00

Page 4: [22] Deleted Martin Morlot 19/02/2023 09:30:00

Page 4: [23] Deleted Martin Morlot 19/02/2023 09:28:00

Page 4: [23] Deleted Martin Morlot 19/02/2023 09:28:00

Page 4: [24] Deleted Formetta Giuseppe 19/02/2023 10:33:00

Page 4: [24] Deleted Formetta Giuseppe 19/02/2023 10:33:00

Page 4: [25] Deleted Morlot, Martin Jean-luc Emile 19/01/2023 09:45:00

Page 4: [25] Deleted Morlot, Martin Jean-luc Emile 19/01/2023 09:45:00

Page 4: [26] Deleted Formetta Giuseppe 19/02/2023 10:36:00

Page 4: [26] Deleted Formetta Giuseppe 19/02/2023 10:36:00

Page 4: [27] Deleted Martin Morlot 19/02/2023 18:11:00

Page 4: [27] Deleted Martin Morlot 19/02/2023 18:11:00

Page 4: [28] Deleted Formetta Giuseppe 19/02/2023 10:37:00

Page 4: [28] Deleted Formetta Giuseppe 19/02/2023 10:37:00

Page 4: [28] Deleted Formetta Giuseppe 19/02/2023 10:37:00

Page 4: [28] Deleted Formetta Giuseppe 19/02/2023 10:37:00

Page 4: [29] Deleted Morlot, Martin Jean-luc Emile 13/01/2023 10:33:00

Page 4: [29] Deleted Morlot, Martin Jean-luc Emile 13/01/2023 10:33:00

Page 4: [30] Deleted Formetta Giuseppe 19/02/2023 10:38:00

Page 4: [30] Deleted Formetta Giuseppe 19/02/2023 10:38:00

Page 4: [30] Deleted Formetta Giuseppe 19/02/2023 10:38:00

Page 4: [30] Deleted Formetta Giuseppe 19/02/2023 10:38:00

Page 4: [30] Deleted Formetta Giuseppe 19/02/2023 10:38:00

Page 4: [30] Deleted Formetta Giuseppe 19/02/2023 10:38:00

Page 4: [30] Deleted Formetta Giuseppe 19/02/2023 10:38:00

Page 4: [30] Deleted Formetta Giuseppe 19/02/2023 10:38:00

Page 4: [30] Deleted Formetta Giuseppe 19/02/2023 10:38:00

Page 4: [31] Deleted Martin Morlot 01/02/2023 19:30:00

Page 4: [32] Deleted Formetta Giuseppe 19/02/2023 10:42:00

Page 4: [32] Deleted Formetta Giuseppe 19/02/2023 10:42:00

Page 4: [33] Deleted Formetta Giuseppe 19/02/2023 10:42:00

Page 4: [33] Deleted Formetta Giuseppe 19/02/2023 10:42:00

Page 4: [33] Deleted Formetta Giuseppe 19/02/2023 10:42:00

Page 4: [33] Deleted Formetta Giuseppe 19/02/2023 10:42:00

Page 4: [33] Deleted Formetta Giuseppe 19/02/2023 10:42:00

Page 4: [33] Deleted Formetta Giuseppe 19/02/2023 10:42:00

Page 4: [33] Deleted Formetta Giuseppe 19/02/2023 10:42:00

Page 4: [33] Deleted Formetta Giuseppe 19/02/2023 10:42:00

Page 4: [33] Deleted **Formetta Giuseppe** **19/02/2023 10:42:00**

Page 4: [33] Deleted **Formetta Giuseppe** **19/02/2023 10:42:00**

Page 4: [33] Deleted **Formetta Giuseppe** **19/02/2023 10:42:00**

Page 5: [34] Deleted **Formetta Giuseppe** **19/02/2023 11:07:00**

Page 10: [35] Formatted **Martin Morlot** **18/02/2023 21:35:00**

Font colour: Auto

Page 10: [35] Formatted **Martin Morlot** **18/02/2023 21:35:00**

Font colour: Auto

Page 10: [35] Formatted **Martin Morlot** **18/02/2023 21:35:00**

Font colour: Auto

Page 10: [35] Formatted **Martin Morlot** **18/02/2023 21:35:00**

Font colour: Auto

Page 10: [35] Formatted **Martin Morlot** **18/02/2023 21:35:00**

Font colour: Auto

Page 10: [35] Formatted **Martin Morlot** **18/02/2023 21:35:00**

Font colour: Auto

Page 10: [35] Formatted **Martin Morlot** **18/02/2023 21:35:00**

Font colour: Auto

Page 10: [35] Formatted **Martin Morlot** **18/02/2023 21:35:00**

Font colour: Auto

Page 10: [35] Formatted Martin Morlot 18/02/2023 21:35:00

Font colour: Auto

Page 10: [35] Formatted Martin Morlot 18/02/2023 21:35:00

Font colour: Auto

Page 10: [35] Formatted Martin Morlot 18/02/2023 21:35:00

Font colour: Auto

Page 10: [35] Formatted Martin Morlot 18/02/2023 21:35:00

Font colour: Auto

Page 10: [35] Formatted Martin Morlot 18/02/2023 21:35:00

Font colour: Auto

Page 10: [35] Formatted Martin Morlot 18/02/2023 21:35:00

Font colour: Auto

Page 10: [35] Formatted Martin Morlot 18/02/2023 21:35:00

Font colour: Auto

Page 10: [35] Formatted Martin Morlot 18/02/2023 21:35:00

Font colour: Auto

Page 10: [35] Formatted Martin Morlot 18/02/2023 21:35:00

Font colour: Auto

Page 10: [35] Formatted Martin Morlot 18/02/2023 21:35:00

Font colour: Auto

Page 10: [35] Formatted Martin Morlot 18/02/2023 21:35:00

Font colour: Auto

Page 10: [35] Formatted Martin Morlot 18/02/2023 21:35:00

Font colour: Auto

Page 10: [35] Formatted Martin Morlot 18/02/2023 21:35:00

Font colour: Auto

Page 10: [35] Formatted Martin Morlot 18/02/2023 21:35:00

Font colour: Auto

Page 10: [35] Formatted Martin Morlot 18/02/2023 21:35:00

Font colour: Auto

Page 10: [35] Formatted Martin Morlot 18/02/2023 21:35:00

Font colour: Auto

Page 10: [35] Formatted Martin Morlot 18/02/2023 21:35:00

Font colour: Auto

Page 10: [35] Formatted Martin Morlot 18/02/2023 21:35:00

Font colour: Auto

Page 10: [35] Formatted Martin Morlot 18/02/2023 21:35:00

Font colour: Auto

Page 10: [36] Formatted Martin Morlot 18/02/2023 21:35:00

Font colour: Auto

Page 10: [36] Formatted Martin Morlot 18/02/2023 21:35:00

Font colour: Auto

Page 10: [36] Formatted Martin Morlot 18/02/2023 21:35:00

Font colour: Auto

Page 10: [37] Formatted Martin Morlot 18/02/2023 21:35:00

Font colour: Auto

Page 10: [37] Formatted Martin Morlot 18/02/2023 21:35:00

Font colour: Auto

Page 10: [37] Formatted Martin Morlot 18/02/2023 21:35:00

Font colour: Auto

Page 10: [37] Formatted Martin Morlot 18/02/2023 21:35:00

Font colour: Auto

Page 10: [37] Formatted Martin Morlot 18/02/2023 21:35:00

Font colour: Auto

Page 10: [37] Formatted Martin Morlot 18/02/2023 21:35:00

Font colour: Auto

Page 10: [37] Formatted Martin Morlot 18/02/2023 21:35:00

Font colour: Auto

Page 10: [37] Formatted Martin Morlot 18/02/2023 21:35:00

Font colour: Auto

Page 10: [37] Formatted Martin Morlot 18/02/2023 21:35:00

Font colour: Auto

Page 10: [37] Formatted Martin Morlot 18/02/2023 21:35:00

Font colour: Auto

Page 10: [37] Formatted Martin Morlot 18/02/2023 21:35:00

Font colour: Auto

Page 10: [37] Formatted Martin Morlot 18/02/2023 21:35:00

Font colour: Auto

Page 10: [37] Formatted Martin Morlot 18/02/2023 21:35:00

Font colour: Auto

Page 10: [37] Formatted Martin Morlot 18/02/2023 21:35:00

Font colour: Auto

Page 10: [37] Formatted Martin Morlot 18/02/2023 21:35:00

Font colour: Auto

Page 10: [37] Formatted Martin Morlot 18/02/2023 21:35:00

Font colour: Auto

Page 10: [37] Formatted Martin Morlot 18/02/2023 21:35:00

Font colour: Auto

Page 10: [37] Formatted Martin Morlot 18/02/2023 21:35:00

Font colour: Auto

Page 10: [37] Formatted Martin Morlot 18/02/2023 21:35:00

Font colour: Auto

Page 10: [37] Formatted Martin Morlot 18/02/2023 21:35:00

Font colour: Auto

Page 10: [37] Formatted Martin Morlot 18/02/2023 21:35:00

Font colour: Auto

Page 10: [37] Formatted Martin Morlot 18/02/2023 21:35:00

Font colour: Auto

Page 10: [37] Formatted Martin Morlot 18/02/2023 21:35:00

Font colour: Auto

Page 10: [37] Formatted Martin Morlot 18/02/2023 21:35:00

Font colour: Auto

Page 10: [37] Formatted Martin Morlot 18/02/2023 21:35:00

Font colour: Auto

Page 10: [37] Formatted Martin Morlot 18/02/2023 21:35:00

Font colour: Auto

Page 10: [37] Formatted Martin Morlot 18/02/2023 21:35:00

Font colour: Auto

Page 10: [37] Formatted Martin Morlot 18/02/2023 21:35:00

Font colour: Auto

Page 10: [37] Formatted Martin Morlot 18/02/2023 21:35:00

Font colour: Auto

Page 11: [38] Deleted Formetta Giuseppe 17/02/2023 17:34:00

1.1.1

Page 11: [39] Deleted Martin Morlot 16/02/2023 09:26:00

Page 15: [40] Deleted Formetta Giuseppe 17/02/2023 20:46:00

Page 24: [41] Deleted Martin Morlot 16/02/2023 11:49:00

Page 29: [42] Deleted Martin Morlot 16/02/2023 18:46:00

Page 29: [43] Deleted Formetta Giuseppe 17/02/2023 19:24:00

Page 29: [44] Deleted Formetta Giuseppe 17/02/2023 19:41:00

Page 29: [45] Deleted **Formetta Giuseppe** **17/02/2023 19:33:00**

Page 29: [46] Deleted **Formetta Giuseppe** **17/02/2023 19:38:00**

Page 29: [47] Deleted **Formetta Giuseppe** **17/02/2023 19:39:00**

Page 29: [48] Formatted **Martin Morlot** **18/02/2023 21:35:00**

Normal

Page 29: [49] Deleted **Formetta Giuseppe** **17/02/2023 19:40:00**

Page 29: [50] Formatted **Martin Morlot** **18/02/2023 21:35:00**

Font: (Default) +Body (Arial)

Page 30: [51] Formatted **Martin Morlot** **18/02/2023 21:35:00**

Font: (Default) +Body (Arial), Font colour: Auto

Page 30: [52] Deleted **Formetta Giuseppe** **17/02/2023 18:33:00**

Page 30: [53] Deleted **Martin Morlot** **16/02/2023 11:08:00**

Page 30: [54] Deleted **Formetta Giuseppe** **17/02/2023 18:36:00**

Page 30: [55] Deleted **Martin Morlot** **16/02/2023 11:05:00**

Page 30: [56] Formatted **Martin Morlot** **18/02/2023 21:35:00**

Font:

Page 30: [57] Formatted Martin Morlot 18/02/2023 21:35:00

Font: (Default) +Body (Arial), Font colour: Auto

Page 30: [58] Formatted Martin Morlot 18/02/2023 21:35:00

Font: (Default) +Body (Arial), Font colour: Auto

Page 30: [59] Deleted Martin Morlot 16/02/2023 11:06:00

Page 30: [60] Formatted Martin Morlot 18/02/2023 21:35:00

Font: (Default) +Body (Arial)

Page 30: [61] Formatted Martin Morlot 18/02/2023 21:35:00

Font: (Default) +Body (Arial)